INVESTIGATING EFFICIENCY AND STABILITY OF GAIT USING A TWO TRIAXIAL IMU SENSOR SYSTEM

by

Joshua Patrick Davies

A thesis submitted to the School of Kinesiology and Heath Studies

In conformity with the requirements for

the degree of Master of Science

Queen's University

Kingston, Ontario, Canada

(May 2020)

Abstract

This work aimed to develop a simple, two-sensor system to measure gait efficiency and stability. The system was tested by measuring the compromised gait pattern of 15 healthy adults (aged 18-30). The gait pattern was altered by forcing participants to walk on their toes on their right side using an ankle-foot orthotic (AFO) and heel wedges. There were 5 conditions: a control condition, a zero AFO condition (AFO with no restrictions or wedges), and a low (5 degrees of plantar flexion), medium (15 degrees of plantar flexion) and high (25 degrees of plantar flexion) wedge conditions. Participants were instrumented with two-sensors, one on their low back, and the other attached to their head, as well as motion tracking markers placed on landmarks of the lower limbs and a motion tracking marker on each sensor. Participants completed ten, 7-meter, walking trials under each condition. Four outcome variables were calculated, two for efficiency and two for stability. The outcome variables were calculated from the movements of the low back and the head and the relationship between them. Repeated measures MANOVAs (Multivariate Analysis of Variance) found an overall decrease in gait efficiency and stability with increasing plantar flexion angle. There was no significant interaction between measurement tool and condition, suggesting that the sensors measured changes in the outcome variables that were similar to those measured by the motion capture system. This work is the first step in the validation of a simple two-sensor system to measure efficiency and stability of gait. Efficiency and stability are two objective and clinically relevant variables that when combined with the tests presently used in clinic will give a more holistic view of an individual's gait.

Acknowledgements

What an incredible journey this has been. My time in Kingston, at Queen's, have been some of the most memorable years of my life, and for that I have so many people to thank:

First, I would like to thank my supervisor, Dr. Pat Costigan. Pat, thank you for your support of my learning and development as a researcher. The way you helped me navigate the development of this project from the beginning is something that I am truly thankful for. You allowed me to develop a project that I was passionate about and provided all the support I needed along the way. I will miss our rants about poorly designed software and our time puzzling over how to get meaningful data from the sensors but will remember them fondly. Thank you for helping me find my passion for research.

To A.J. Ventor and his team at V2Inovations, thank you for designing and donating the orthotics for my project. Your passion for research and innovation is something that I admired from the first time we met. Thank you for your support.

Megan, your willingness to help unconditionally with data collection, whether it be pilot work or otherwise, was simply amazing. I couldn't have gotten through it all without you, or at the very least it might have taken me an extra year and it sure wouldn't have been as fun. You are a talented researcher and I can't wait to see where your career takes you. As my master's spilled over into a third year, I would also like to thank you and Ryan for graciously hosting me whenever I needed a place to stay in Kingston.

Tara and Tom, what fun we had in Kingston. I will remember the hangouts, the Mario Kart and great food. You are both a great example of individuals that are willing to go out of their way to help their friends. The time I spent at your place on a nearly nightly basis was part of what made my time in Kingston so amazing. It is tough that life has put nearly 9 hours of driving between us, but I look forward to many future visits!

Spencer, Rob and Markus, thank you for being great lab-mates and friends. From grinding out long workdays in the lab, to lunches out, to running tutorials you helped make my experience at Queen's an enjoyable one.

Mom and Dad thank you for your support through this whole process financially and otherwise. Your patience and understanding are second to none and I would like to extend my most heartfelt thank you. You instilled values of dedication, hard work and a little stubbornness in me, that have certainly helped throughout this journey.

Finally, to the love of my life, biggest supporter, and wife Émilie, so much has changed for us in the last few years. It has been quite an adventure, from our engagement on the rocks down by the St. Lawrence River to all your visits to see me and my friends in Kingston. Kingston and the people we have met here will always be a special part of our life together. Thank you for your encouragement, support and understanding. I know getting this thesis finished took longer than I had planned, but you were always supportive and loving. I am so lucky to have your love and support for the rest of my life.

Table of Contents

List of Figures

List of Tables

List of Abbreviations

AFO Ankle-Foot Orthotic

BEQ Biomechanical Efficiency Quotient

CoM Center of Mass

FFT Fast Fourier Transform

HAT Head, Arms and Trunk

HR Harmonic Ratio

IMU Inertial Measurement Unit

PCA Principle Component Analysis

Chapter 1

Introduction

Moving from place to place is essential in everyday life and, for the general population, walking is often thought to be an effortless and unconscious task. Several biomechanical aspects of the normal gait pattern make it efficient, which is why individuals can walk at their naturally selected walking speed for long periods of time (Perry, 1992). When the normal gait pattern is altered, walking requires more effort and is more taxing (Van Den Hecke et al., 2007). Many clinical populations have an altered gait pattern, where some deficit, whether it be to the sensory or motor systems, or a physical impairment, alters the way they walk. Current human gait research provides insight into the underlying factors that cause less efficient gait patterns, yet it is hard to make quantitative measures of gait in a clinical setting.

The clinical analysis of populations with pathological gait patterns relies heavily on a qualitative analysis by clinical professionals (Bache, Selber, & Graham, 2003). Often the clinical professional watches the patient walk and comments on the abnormalities of their gait. These subjective comments may be supplemented by passive range of motion measurements taken using a goniometer. Other clinical assessment tools such as the Timed Up and Go, the Six Minute Walk test, and the Observational Gait scale (American College of Rheumatology, 2015; Carey, Martin, Combs-Miller, & Heathcock, 2016; Mackey, Lobb, Walt, & Stott, 2003) are used but provide little insight to the abnormalities that alter gait performance and what treatment(s) would be most effective at improving performance.

The standard used to quantify gait characteristics is a session in a gait laboratory equipped with motion capture cameras, force plates and electromyographic sensors and allows for a more complete assessment of gait compared to a visual gait assessment alone (Saleh & Murdoch, 1985; Wren et al., 2005). A systematic review of gait analysis found that when gait analysis was used as

a tool to make informed treatment decisions, those treatments were used and successful a high percentage of the time (Wren, Gorton, Õunpuu, & Tucker, 2011). While it has been suggested that factors such as: availability, reimbursement from insurance companies, and education are barriers to a more consistent use of gait analysis (Wren et al., 2011), perhaps a simplified tool to provide objective measures in the clinic would either: (1) provide an initial screening tool to support the use of a full gait assessment. Or, (2) provide enough detail when combined with visual observation to support the use of specific treatment protocols.

Human gait can be reduced to four main subtasks: a) movement toward the destination, b) maintaining equilibrium while moving, c) adapting to changes in the environment, and d) initiating and terminating locomotion (Woollacott & Tang, 1997). Extrapolating on subtask (a) it is desirable that movement toward the destination be as efficient as possible; allowing an individual to cover the most distance with the least energetic cost. Subtasks (b) and (c) relate to the body's stability as it moves. An individual must be able to keep themselves in equilibrium and respond to changes in the environment to safely progress toward their destination. Given that both efficiency and stability are key components of gait, and that these components are compromised in clinical populations (Benda, Smith, & Lange, 2002; Menz, Lord, & Fitzpatrick, 2003b; Ries & Schwartz, 2017), measurements of efficiency and stability would be useful when exploring gait in a clinical setting.

This work aimed to provide a simple, two IMU (Inertial Measurement Unit) sensor system to measure gait efficiency and stability. The system was tested by altering the gait pattern of an able-bodied population. The gait pattern was compromised by forcing varying degrees of plantar flexion on the right side using an (Ankle-Foot-Orthosis) AFO and heel wedges. It was hypothesized that: (1) there will be a measurable change in gait stability and efficiency with increasing plantar flexion angle; and (2) IMU sensors will measure similar changes in stability and efficiency when compared to a motion tracking system.

If effective, this system would provide a quick, cost effective and easy to use tool needed to quantify and analyze clinical gait patterns and without having to visit a specialized gait laboratory.

Chapter 2

Literature Review

2.1 Gait

To understand the mechanics of gait, it is important to know how the gait cycle is described. Normal walking is a series of controlled, coordinated and repeated flexions and extensions of the hip, knee, and ankle joints but because of its cyclical nature there is no definite beginning and end to the gait cycle. However, the most common gait event used to define the beginning and end of a stride is heel-strike. Therefore, one stride cycle can be defined by the heel-strike of one foot to the subsequent heel-strike of that same foot. A stride cycle is divided into two main phases: stance phase and swing phase. During the stance phase the foot is in contact with the ground and during the swing phase the foot is off the ground and moving towards its next heel contact. The stance phase is approximately sixty percent of a stride with the swing phase making up the remaining forty percent (Murray, 1967).

The main objective of gait is to advance the body's mass in the desired direction. To do so the upper body needs to remain balanced and supported. The top-heavy nature of the human body combined with the multi-segmental lower limbs, and the contours of the hip, knee and ankle joints make maintaining stability a challenge. Keeping the upper body positioned over the legs is the most important contributing factor in maintaining total body stability while standing and walking (Perry, 1992). A common model that describes how the body moves is the 'passenger-locomotor' model. This model identifies the head, arms and trunk (HAT) as the passenger and the legs as the locomotor (Perry, 1992). The main responsibility of the passenger is minimizing extraneous movement of the HAT over the legs to create an energy efficient gait. If the HAT stays aligned over the base of support (the legs), then the muscle activity required by the HAT to remain stable is minimized (Perry, 1992).

The legs are the ‘engine’ that provides the strength to move the body forward. Each of the legs takes a turn supporting the passenger and providing the force required to progress the HAT. Upon heel strike, the leg absorbs the force from the natural fall of the HAT. Once this force has been absorbed there is a progression of the body over the foot. The progression of the body over the stance foot is best described using the concepts of ‘heel rocker’, ‘ankle rocker’ and ‘forefoot rocker’. A rocker describes a pivot point for the HAT, and the smooth progression from the heel rocker to the forefoot rocker is in part what makes walking efficient, as minimal muscular effort is required and much of the body’s forward momentum is conserved.

When the heel hits the ground the knee and hip flex slightly to absorb the force of impact. The heel helps to preserve the forward momentum of the body that has been gained by the forward fall of the HAT by acting as a rocker. Then the foot passively plantarflexes and the forefoot contacts the ground. Once the mid-foot is in contact with the ground, the ankle then serves as the pivot point. Because the foot is stationary, the tibia rotates about the ankle in passive ankle dorsi-flexion maintaining the body’s forward momentum (Perry, 1992). The soleus and gastrocnemius muscles are important in this stage of gait. As the tibia rotates forward, the soleus contracts to make the tibia a stable base for knee extension (Perry, 1992). This contraction of the soleus, with help from the gastrocnemius, helps stabilize the knee, but also helps control the anterior rotation of the tibia at the ankle allowing the body to further progress over the stance foot (Perry, 1992). Next, the center of pressure of the ground reaction force moves anterior to the knee, causing knee extension as the body progresses over the stance foot (Gage, 1993). The last phase of the progression is when the center of pressure reaches the metatarsals and the heel begins to rise from the ground. Because the contralateral foot has not yet contacted the ground and the body has progressed over the stance foot, the body’s center of mass (CoM) is outside of the base of support, causing the body to become unstable. As the body mass rotates about the forefoot rocker and begins to fall forward, it is caught by the contralateral foot at its heel strike (Perry, 1992).

The forefoot rocker and the added push-off force by the plantar flexors puts the foot in the position to begin the swing phase as the weight is transferred to the contralateral foot, now in mid-stance. The rectus femoris contracts to flex the hip and swing the leg forward, passing by the stance foot as it reaches for the ground. The knee then extends and the ankle dorsiflexes to prepare for the next heel contact. This forward swing of the leg also provides forward momentum to help the body progress over the stance foot.

The gait patterns described above are expected in an able-bodied population. When normal gait is compromised, whether it be from a disability, or a forced intervention (such as in this work), several biomechanical aspects of gait will be affected.

2.2 Effect of Forced Plantar Flexion and Limited Dorsiflexion on Normal Gait

The intervention used to alter normal gait included two changes to the participants' right side: (1) varying the degree of forced plantar flexion and (2) restricted dorsiflexion (refer to Chapter 4 for more detail; pg. 38). These two interventions can cause several biomechanical changes to the gait patterns described in the previous section.

First, an increase in the ankle's forced plantar flexion angle reduces the ability to push off. In able-bodied individuals forced into a plantar flexion angle of greater than twenty degrees, a fifty percent decrease in ankle power during push-off was reported (Houx, Lempereur, Rémy-Néris, & Brochard, 2013). The reduction in power is likely because the plantar flexors had less range over which to generate force (Manning, 2005).

The forced plantar flexion and limited dorsiflexion also alter the swing phase of the affected side. When the ankle's dorsiflexion range is restricted and the walker's foot cannot clear the ground effectively, different strategies are needed to achieve foot clearance (Bennett et al., 2005). Hip flexion and anterior pelvic tilt angles increase significantly when dorsiflexion range is limited to less than ten degrees (Houx et al., 2013). Subsequently, the increased pelvic tilt will cause greater vertical excursion of the body's center of mass during swing phase.

Finally, the unaffected limb needs to compensate for the asymmetry between the left and right sides caused by the increased plantar flexion angle on the affected side. On the unaffected side, knee flexion and ankle dorsiflexion decrease during swing phase and ankle power absorption increases at initial contact (Houx et al., 2013). The increase in power absorption may be a result of increased velocity of the body's CoM as it falls from a greater height after going 'up and over' the plantarflexed side.

The above changes to the kinematics and kinetics of normal gait will cause changes in the overall efficiency and stability of gait. Efficiency and stability, and how they are affected by these kinematic and kinetic changes to gait, will be discussed in the following sections.

2.3 Energy Trade-Off and Walking Efficiency During Gait

Gait efficiency can be defined as the amount of useful work that is done by a given amount of physiological energy (Perry, 1992; Ries & Schwartz, 2017). The benefits of energy recovery and avoiding erratic extra movements of the body's center of mass may help reduce the overall metabolic cost of walking while achieving the same amount of useful work, therefore making gate more efficient. The inverted pendulum model is an early model of gait that helps explain how energy is recovered throughout the stride cycle.

The main mechanism required to make walking efficient is the control of the body's CoM (Perry, 1992). Human gait, specifically the movement of the body's CoM, has been compared to an inverted pendulum (Cavagna, Heglund, & Taylor, 1977). As it swings, a pendulum's energy changes from gravitational potential energy in the most upward position to kinetic energy in the downward swing. Much like the pendulum, there is a transition from gravitational potential energy to kinetic energy as the body's CoM falls from its high point in midstance to a low point at heel strike. From midstance to heel strike, the body's CoM is moving downward and forward. This forward and downward motion causes an increase in body's CoM velocity and the conversion of potential energy to kinetic energy. Once heel strike of the contralateral foot occurs (the CoM's

minimum height occurs just after heel strike) and the body starts to progress over the new stance leg, the body's CoM rises until its peak at midstance (Figure 2.1). This forward and upward motion causes a decrease in body's CoM velocity as it rises with the conversion of kinetic energy to potential energy. At this point the potential energy of the CoM is at its peak, and the cycle repeats.

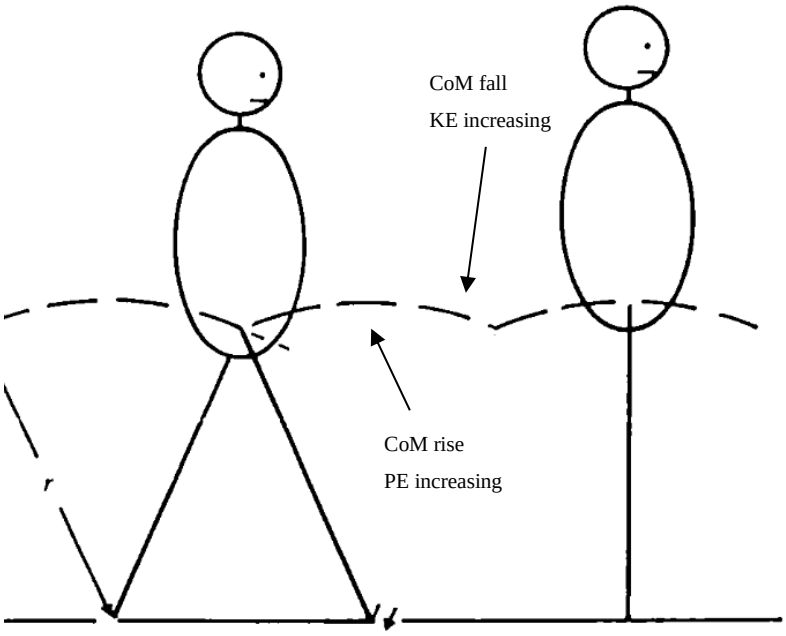

Figure 2.1: Center of mass displacement during gait. Center of mass is at a high point during mid-stance and a low point at heel strike. (Adapted from Winter, 1979).

The kinetic and potential energy profiles are almost mirror images of each other (Figure 2.2) and the resulting total energy profile is the sum of the potential and kinetic energies (top line in Figure 2.2). The total energy change throughout the gait cycle is less than the energy change in either of the potential or kinetic energies. For the energy level of the body to change some force is required, therefore, keeping the energy changes to a minimum reduces the mechanical work requirements of walking. However, walking at a normal speed still demands approximately 30-40% of an average individual's maximal oxygen uptake (Lazzer et al., 2005; Perry, 1992). If a

person is working at 30-40% of their maximal oxygen uptake, there is still mechanical work being done by the legs on the CoM to make locomotion possible (Cavagna & Kaneko, 1977). For this reason, the simplicity of the inverted pendulum model has been challenged in more contemporary gait research. The Dynamic Walking Model considers the inverted pendulum model and adds to it.

The Dynamic Walking Model considers the walking body as an inverted pendulum while adding that walking is not a 'zero-cost' activity (Kuo, 2007). The Dynamic Walking Model adds to the inverted pendulum model by considering the step-to-step transition (Kuo, 2007). The body can only truly be modelled as an inverted pendulum during the single-leg support phases. During the step-to-step transition, negative work is done by the leading leg and positive work is done be the trailing leg. Because the forces of the leading and trailing leg are acting in opposite directions, the step-to-step transition is inherently costly. The push-off force generated by the trailing leg is important to compensate for the energy lost due to the backward acceleration at heel strike. The collision between the swing foot and the ground is modelled as an inelastic collision (Kuo, 2007). The energy lost from the inelastic collision can be reduced by up to 75% by applying a push-off force from the contralateral leg (Kuo, 2007). With that considered, the coordination of heel strike and push-off and short duration of the transition are imperative to energy conservation. If an individual walks with increased plantar flexion, whether from a forced intervention or a physical impairment, they are not able to generate as much force at push off. The reduced ability to generate force from the trailing leg causes a less efficient gait pattern, as they are able to regenerate the energy lost from heel strike effectively (Huang, Shorter, Adamczyk, & Kuo, 2015).

The energy of the CoM and the step-by-step transition can be drastically different in a clinical population (Bennett et al., 2005). For example, the kinetic-potential energy trade-off is less efficient in the cerebral palsy population, with thirty-three percent less energy recovered from one stride to the next (Bennett et al., 2005) which increases the metabolic cost of gait as more mechanical work has to be done to compensate for the energy loss. The metabolic cost of walking

for someone with cerebral palsy is two to three times higher than the metabolic cost for an able-bodied individual (Bolster, Balemans, Brehm, Buizer, & Dallmeijer, 2017; Duffy, Hill, Cosgrove, Corry, & Graham, 1996; Kurz, Stuberg, & DeJong, 2010; Norman, Bossman, Gardner, & Moen, 2004; Ries & Schwartz, 2017). This increase in metabolic demand is likely due to: an increase in the body's CoM vertical displacement, over and above what is necessary for pendular motion (Bennett et al., 2005), muscle spasticity and uncoordinated muscle activation patterns (Ries & Schwartz, 2017).

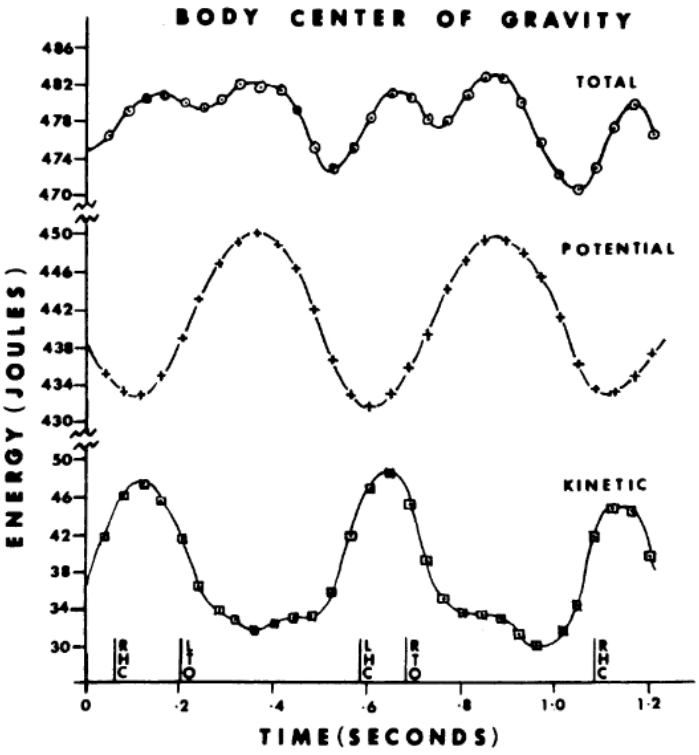

Figure 2.2: Kinetic and potential energy profiles of the CoM in normal gait and their sum. The kinetic and potential energies are a 180-degree phase shift from one another with similar amplitudes. The sum of the energies is fairly constant demonstrating the efficiency of the trade-off between kinetic and potential energies (Winter, 1979).

When discussing mechanical and metabolic energy, it is important to understand their similarities and differences. Mechanical energy and metabolic energy are correlated (Jones & McLaughlin, 1993; Peyrot et al., 2009), but mechanical energy does not account for some variables that affect metabolic cost. Co-contraction of muscles, the metabolic efficiencies of different types of muscle contractions, energy storage in muscles and passive tissues and maintenance of balance are all reasons why mechanical energy costs and metabolic energy costs differ in walking (Burdett, Skrinar, & Simon, 1983; Donelan, Shipman, Kram, & Kuo, 2004; Menard, Penn, Lee, Dusik, & Hall, 1991). With the differences between metabolic and mechanical energies considered, mechanical variables such as work, and center of mass motion can still provide some insight into the overall metabolic cost of walking. The mechanical work done to move CoM accounts for roughly fifty-percent of the metabolic cost of walking (Duff-Raffaele, Kerrigan, Corcoran, & Saini, 1996a), supporting the use mechanical efficiency to draw conclusions about the overall cost of walking. Quantifying mechanical efficiency would provide insight to the efficacy of treatment programs and give clinicians additional information to help guide decisions on whether to change or keep their current treatment modalities.

2.4 Gait Stability

Gait stability can be defined as the ability to keep balance when posture is perturbed (Latash, 2012). Stability is directly related to subtasks b and c of the four subtasks of gait; (c) maintaining equilibrium while moving, and (d) adapting to changes in the environment (Woollacott & Tang, 1997) . An individual must be able to maintain equilibrium while continuing to move forward and adapting to the challenges of the environment around them which may perturb their posture. Clinical populations often are at an increased falls risked due to their lack of ability to perform these two subtasks that are vital to maintaining stability while walking (Woollacott & Tang, 1997).

The challenge of maintaining balance while moving is much more complex than staying balanced while stationary. While stationary, all that is required for an individual to stay balanced

is to maintain their CoM within their base of support (Perry, 1992). This is done by moving the body's CoM since the base of support is stationary. When an individual begins to move, the challenge becomes that both the CoM and the base of support are moving. Specifically, during the single leg support phase, the body's CoM is not always within the base of support (Woollacott & Tang, 1997), putting the body in a situation where it is required to 'catch itself from falling'. The torque created by gravity acting on the body's CoM during the weight shift from one side to the other needs to be counter-balanced by a hip and lower trunk torque to prevent the body from falling (Winter, 1979). Therefore, when shifting the weight from one limb to the next, the projection of the CoM laterally must be predicted so that once the weight shift is completed the CoM is within the new base of support. The complexity of dynamic stability continues to build as the forward progression of the body must also be considered. Heel strike and push off are two instances where it is hard to maintain stability in the anterior-posterior directions as the large backward acceleration at heel strike causes the head, arms and trunk to fall forward, and the large forward acceleration caused by push-off causes the head, arm and trunk to fall backward. Muscle moments about the hip must be generated to counteract this forward and backward motion of the HAT (MacKinnon & Winter, 1993). In the anterior-posterior direction, the body's CoM falls outside of the base of support sometime between one single limb support phase and the next double limb support phase. Proper foot placement is imperative to 'catch' the falling body and reestablish the body's CoM within the base of support. Controlling the motion of the upper body allows for the body to remain stable during walking.

When an individual is forced into varying degrees of plantar flexion on one side, stability is affected because the gait pattern becomes unfamiliar (Mignardot et al., 2014). The change in the gait pattern may make it more difficult for the individual to predict their body's CoM trajectory both in the forward and mediolateral directions. Furthermore, the requirement to for the body to move 'up and over' the plantarflexed foot on the right side will likely cause greater accelerations

that may perturb posture and make gait less stable. The effects of forced plantar flexion on one side of the body discussed above are likely also present in clinical populations (Houx et al., 2013). It is important for clinicians to accurately assess gait stability so that they can more effectively help their patients.

The efficiency and stability of gait are two clinically relevant measures. Current observational measurement tools such as: The Dynamic Gait Index, The Functional Gait Assessment and the Timed Up and Go test either lack the ability to measure these variables objectively or fail to provide insight into the underlying causes of decreased stability or efficiency. These common observational measurement tools and others will be discussed in the following paragraphs.

2.5 Observational Measurement Tools

There are several analysis tools that are used to evaluate gait in a clinical setting. Although they do not provide the detailed analysis that can be achieved in a gait laboratory, they have strong interrater reliability and provide a starting point for quantifying gait. Common tools used in the clinic include: The Dynamic Gait Index, Functional Gait Assessment, Six-minute Walk test, Timed Up and Go, and the Observational Gait Scale.

The Dynamic Gait Index evaluates functional stability during gait activities with the goal of evaluating the risk of falling (Shumway-Cook, Baldwin, Polissar, & Grubar, 1997). The Dynamic Gait Index tests: walking while changing speeds and turning the head, pivot turns, and stair climbing (Jonsdottir & Cattaneo, 2007). The Dynamic Gait Index was created to help identify the risk of falling in the elderly, but it is useful in clinical populations as well individuals who have suffered a stroke and people with multiple sclerosis (Jonsdottir & Cattaneo, 2007; McConvey & Bennett, 2005). The Functional Gait Assessment is an extension of the Dynamic Gait Index that adds three additional functional evaluations: gait with a narrow base of support, walking backwards, and walking with eyes closed (Wrisley, Marchetti, Kuharsky, & Whitney, 2004). The rational of adding these three new evaluations was to make the test more applicable to people with

vestibular disorders (Wrisley et al., 2004). The Functional Gait Assessment, like the Dynamic Gait Index has good interrater and intra-rater reliability and is easily administered in a clinical setting (Wrisley et al., 2004).

The Six-Minute Walk test was originally used clinically to test the aerobic capabilities of people with chronic obstructive pulmonary disease (Maher CA, Williams MT, Olds, 2008). The Six-Minute Walk test involves the client walking around a thirty-meter circuit for six minutes. A lesser distance covered is representative of lower function (American College of Rheumatology, 2015a). The Six-Minute Walk test is not a direct evaluation of gait characteristics, although it is likely that an individual who covers a lesser distance during the test is using a less efficient gait pattern compared to an individual who covers more distance. This test is becoming increasingly more popular to evaluate the functional ability of people with cerebral palsy and has been shown to be a valid and reliable measure (Maher CA, Williams MT, Olds, 2008). The Six-Minute walk test is a valuable tool because it is easy to administer and easily repeatable which makes it a good candidate to be used in a clinical setting.

The Timed Up and Go test is another easily administered clinical test used to evaluate mobility. It was originally used to detect falls risk in the elderly (American College of Rheumatology, 2015b), but is useful in evaluating individuals with cerebral palsy (Carey, Martin, Combs-Miller, & Heathcock, 2016). To administer the Timed Up and Go, all that is required is a chair and approximately three meters of space. The client is asked to rise from the chair walk three meters forward, then return to the chair. The amount of time taken is the measure of an individual's mobility, with a greater time to completion representing lesser mobility (American College of Rheumatology, 2015b). The Timed Up and Go test accurately differentiates between categories on the Gross Motor Function Questionnaire, a tool to classify the gross motor function of individuals with cerebral palsy (McDowell, 2008). The Timed Up and Go is a valid and reliable measure of mobility that is easy to administer in a clinical setting (Carey et al., 2016). Like the Six-Minute

Walk test, the Timed Up and Go does not measure gait characteristics directly but can be used to make inferences on attributes of gait such as efficiency and stability. An individual who takes more time to complete the Timed Up and Go test is likely walking less efficiently. Furthermore, a longer Timed Up and Go result is indicative of less dynamic stability and a greater falls risk (Bonnyaud, Pradon, Bensmail, & Roche, 2015; Jones & McLaughlin, 1993; Shumway-Cook, Baldwin, Polissar, & Grubar, 1997).

The Observational Gait Scale (Boyd & Graham, 1999) is adapted from the Physician's Rating Scale. The scale is a scoring system that guides clinicians in their evaluation of characteristics such as the degree of knee flexion during stance phase and the position of the foot during initial contact. Once each of the categories have been scored, the sum of the scores is calculated to give a cumulative score. The lower the number the less normal an individual's gait pattern. This is a valuable clinical tool because it scores specific aspects of gait making it consistent across administrators. The Observational Gait Scale has been shown to be reliable when evaluating the gait of older children with cerebral palsy (Mackey, Lobb, Walt, & Stott, 2003). This tool provides some structure to observational gait analysis while attempting to quantify the quality of gait patterns in clinical individuals.

The clinical tools and assessments described above are some of the more commonly used assessment tools in clinical practice. While some of these tests provide objective measures of gait, they are limited by the conclusions that can be drawn from their results. Inertial measurement unit (IMU) sensors seem to be the next logical step in the attempt to bring quantitative gait analysis to the clinic. These sensors are small and cost effective and will allow more direct measures of gait efficiency and stability to be obtained in the clinical setting.

2.6 Sensors

Wearable sensors have great potential as clinical tools (Tao, Liu, Zheng, & Feng, 2012). A single sensor has been used to measure gait stability in the elderly and other clinical populations

(Buckley, Galna, Rochester, & Mazzà, 2015; Latt, Menz, Fung, & Lord, 2008; Menz, Lord, & Fitzpatrick, 2003c, 2003a; Tamura, 2005) or by adding more sensors to the system, may be used to estimate joint angles and limb displacements (Tao et al., 2012). When using sensors for gait measurement, it is usually better to use a sensor that provides several different measurements. Currents sensors available for gait analysis include accelerometers, gyroscopes, magnetometers and more (Tao et al., 2012). The functionality of accelerometer sensors and their applications will be discussed.

An accelerometer is a sensor that contains a small, known mass that measures accelerations along a single axis. In an accelerometer, inertial forces due to gravity or motion cause the mass to accelerate which changes the accelerometer's internal configuration. The change in configuration is proportional to the applied inertial force (F) that is equal to the mass multiplied by the acceleration (ma). Since the mass is known, the equation F= ma is used to solve for the acceleration (Tao et al.). Today's accelerometers sensors usually contain three individual accelerometers positioned at right angle to each other to measure three-dimensional accelerations.

When an accelerometer is attached to the body's low back and the top of the head, the recorded acceleration patterns can be used to calculate gait stability and efficiency measures (Buckley et al., 2015; D. Kerrigan, Thirunarayan, Mandyam Sheffler, Ribaudo, & Corcoran, 1996; Menz et al., 2003b; Menz, Lord, St George, & Fitzpatrick, 2004). Measures of gait stability can be calculated directly from the acceleration signal by preforming a harmonic analysis and calculating the harmonic ratio and the RMS of the acceleration signal (Buckley et al., 2015; Menz et al., 2003c; Smidt, Arora, & Johnston, 1971). Calculating gait efficiency measures often involves processing the acceleration to calculate velocity and displacement. Once the velocity and displacement information are available variables related to gait efficiency, such as kinetic and potential energies of the low back, can be calculated.

One of the driving reasons to maintain an efficient gait is to conserve energy. Therefore, a more efficient gait pattern will optimize the trade-off between kinetic and potential energy of the body's CoM. As described in a previous section, an efficient gait pattern displays a one hundred and eighty degree phase shift between kinetic and potential energies of the CoM (Bennett et al., 2005; Perry, 1992). A cross-correlation, a value between negative one and one, is a measure of the likeness of two curves. A cross-correlation value of one represents two curves that are perfectly in phase and a correlation of negative one represents two curves that are perfectly inverse to one another. Kinetic energy is calculated from the anterior-posterior velocity while potential energy is calculated from the vertical displacement. Since, in the kinetic energy formula (Equation 1), the one-half constant, mass of the object, and the square on the velocity term are simply scalar multiples they only effect the amplitude of the curve not its phase. Likewise, in the potential energy formula (Equation 2), mass and gravity, are scalar multiples and only effect the amplitude of the curve, not its phase. As such, the cross-correlation between these energy profiles will not be affected if these terms are removed. Therefore, for simplicity, the cross-correlation can be calculated by cross-correlating the vertical displacement and forward velocity. The cross-correlation value provides a measure of gait efficiency, as a more coordinated energy trade-off at the CoM will help reduce the overall cost of walking. In a population of individuals with cerebral palsy, an average phase shift (shift of the curves in time) from kinetic to potential energy of the CoM of 135 degrees was observed compared to a 165 degree phase shift in between CoM energies in the control population (Bennett et al., 2005). The difference in phase would be apparent in the cross-correlation values as they would be less negative (mathematically increased).

Equation 1: Kinetic energy formula.

$$KE = \frac{1}{2}mv^2$$

Where:
$m = mass$
$v = velocity$

Equation 2: Potential energy formula.

$$PE = mgh$$

Where:
$m = mass$
$g = gravity$
$h = height\ from\ the\ ground$

The Biomechanical Efficiency Quotient (BEQ; Kerrigan et al., 1996) indirectly relates the mechanical costs of walking to the metabolic costs. The BEQ is a second measure of the efficiency of gait that can be computed from the data produced by an accelerometer (D. Kerrigan et al., 1996). The BEQ equation requires three variables: the vertical displacement of the CoM, the average stride length and the sacral height. The quotient (Equation 3) is calculated as a ratio of the measured vertical excursion of the CoM to the predicted vertical excursion of the CoM (Equation 4). The BEQ is a measure of gait efficiency as a greater BEQ represents a gait pattern where the CoM is moving more than is necessary for normal efficient gait. The unnecessary extra movements of the center of mass have been shown to be more metabolically costly (Gordon, Ferris, & Kuo, 2009). The quotient proved accurate enough to differentiate between normal individuals and those with cerebral palsy, and further, differentiated between persons with spastic diplegia or spastic hemiplegia (D. Kerrigan et al., 1996).

Equation 3: BEQ formula. The ratio between measured vertical CoM excursion and predicted vertical CoM excursion

$$BEQ = \frac{m}{p}$$

Where:
$BEQ\ is\ the\ Biomechanical\ efficiency\ quotient$
$m\ is\ the\ measured\ center\ of\ mass\ excursion$
$p\ is\ the\ predicted\ vertical\ center\ of\ mass\ excursion$

Equation 4: Vertical CoM excursion prediction formula.

$$p = \frac{1}{2}(h - \sqrt{h^2 - \left(\frac{1}{4}l\right)^2})$$

Where:
$p\ is\ the\ predicted\ vertical\ center\ of\ mass\ excursion$
$h\ is\ the\ sacral\ height$
$l\ is\ the\ average\ stride\ length$

The acceleration patterns of the head and low back and the relationship between them can be used to calculate measures of dynamic stability (Buckley et al., 2015; Menz et al., 2003a, 2003b; Menz, Lord, et al., 2004; Smidt, Deusinger, Arora, & Albright, 1971). Because human gait is bipedal, we expect accelerations to occur in multiples of two during a stride cycle. The braking at heel strike causes two distinct acceleration patterns and we expect these patterns to occur in multiples of two, as there are two heel strikes per stride. If an acceleration pattern does not occur as a multiple of two, it is considered an irregular acceleration pattern and represents a less stable gait pattern (Menz et al., 2003b). Overall gait stability can be represented by a harmonic ratio value (Menz et al., 2003c). To calculate the harmonic ratio the acceleration signal is decomposed into its harmonic parts using a finite Fourier transform. Even number harmonics are representative of patterns that happen in multiples of two and odd numbered harmonics represent harmonic patterns

that are not finished within a stride cycle. The harmonic ratio is created by dividing the sum of the even numbered harmonics and the sum of the odd numbered harmonics. A higher harmonic ratio represents a more stable walking pattern (Menz et al., 2003b).

The harmonic ratio has been used in many studies to quantify dynamic gait stability (Menz, Latt, Tiedemann, Kwan, & Lord, 2004; Menz et al., 2003b, 2003c, 2003a; Menz, Lord, et al., 2004) For example, a 2003 study examined the difference in the dynamic stability of older and younger adults (Menz et al., 2003c). The participants were instrumented with an accelerometer on their lower back and preformed two walking trials on each of four different surfaces (normal and on different unpredictable surfaces). Older adults known to be at risk of falling had a lower harmonic ratio than a healthy young adult population while older adults with no fall risk had no difference in their harmonic ratio values compared to the healthy young adult population (Menz et al., 2003a). This suggests that the harmonic ratio stability metric can be used measure stability and correctly identify less-stable populations.

Additionally, the attenuation of acceleration amplitude (calculated from root-mean-square (RMS)) from the low back to the head can be a measure of an individual's stability during gait. Since a main requirement of locomotion is to keep the head stable for the purposes of gaze orientation (Pozzo, Berthoz, Lefort, & Vitte, 1991), the accelerations should be attenuated from the low back to the head. Table 2.1 displays RMS values of the head and low back accelerations of a control population and a population of people with Diabetic Peripheral Neuropathy (considered to have a less stable gait). In most cases the individuals with Diabetic Peripheral Neuropathy (DPN) displayed smaller attenuation values compared to the control population. Other studies have also reported acceleration attenuation from the low back to the head (Buckley et al., 2015; Menz et al., 2003b; Prince, Winter, Stergiou, & Walt, 1994). The acceleration attenuation is most apparent in the mediolateral and anterior-posterior direction.

Table 2.1: RMS acceleration values of the center of mass and the head, comparing the normal population to the DPN population walking on level and irregular surfaces (Adapted from Menz et al., 2004).

			Pelvis RMS (g)	Head RMS (g)	% Attenuation
Control	Level Surface	Vertical	.203±.05	.183±.04	10
		AP	.158±.03	.139±.03	15
		ML	.155±.05	.126±.04	18
	Irregular	Vertical	.215±.05	.177±.05	17
	Surface	AP	.187±.04	.161±.04	14
		ML	.196±.06	.133±.03	32
DPN	Level Surface	Vertical	.173±.04	.139±.04	20
		AP	.131±.03	.137±.02	-5
		ML	.129±.03	.126±.04	2
	Irregular	Vertical	.170±.05	.124±.04	27
	Surface	AP	.138±.04	.157±.03	-14
		ML	.146±.04	.128±.03	12

An accelerometer can be useful in a clinical setting. Yet, there are factors that limit using these measurement tools in the clinic to evaluate gait. Finding the best strategy to process acceleration data to calculate velocity and displacement while limiting the effects of drift cause by signal noise and movement artifact remains challenging. Several different processing techniques will be explored in the next chapter.

Chapter 3

Sensor Processing

3.1 The Inertial Measurement Unit (IMU)

For this project, two MetaMotion-r3 IMU sensors (mbientlab, San Francisco CA) were used. These sensors are equipped with accelerometers, gyroscopes, and magnetometers. The local coordinate system for the IMU is shown in Figure 3.1. With some onboard processing these sensors output linear acceleration and the gravity vector, which are the two outputs that were used in this project. These two outputs result from separating the total acceleration into two components: acceleration caused by motion (linear acceleration), and acceleration due to gravity. Figure 3.2 shows the low back sensor on a participant. All processing methods discussed in this chapter refer to the low back sensor.

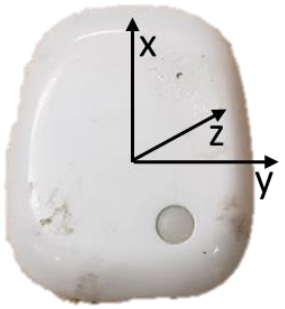

Figure 3.1: Close up of MetaMotion-r3 sensor with its local coordinate system defined.

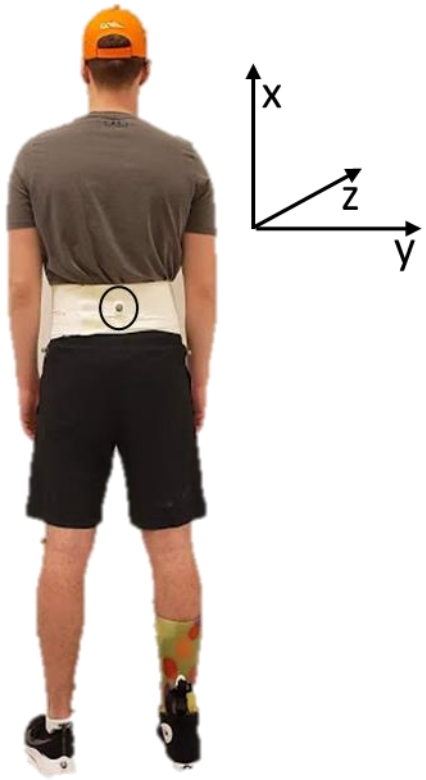

Figure 3.2: Participant instrumented with the low back, IMU sensor (circled). The local coordinate system of the low back, IMU sensor is shown using the black axes, where x is vertical, y is mediolateral, and z is fore-aft.

3.2 Sensor Acceleration Processing Methods

Processing the acceleration to calculate velocity and displacement was one of the biggest challenges of the project. Small inaccuracies in acceleration led to large inaccuracies in velocity and even larger inaccuracies in displacement. The presence of 'drift' in the acceleration signal made it difficult to differentiate between the acceleration caused by 'real movement' and acceleration caused by artifact/signal noise. During integration, the erroneous 'drift' in the acceleration signal is included in both the computed velocity and displacement. Several acceleration processing methods were explored in hopes of finding a process that mitigates the effects of drift. These processing techniques will be discussed briefly in the following paragraphs.

3.2.1 Mathematical Integration

Standard mathematical integration was the first method explored to calculate velocity and displacement in all three axes directions (Y-side-to-side, Z-fore-aft , X-vertically). This method is affected by drift in the acceleration data. A small error in the acceleration measurement causes an error when integrating to compute velocity and an even greater error when integrating velocity to compute displacement. For example, Figure 3.3 shows the acceleration and resultant velocity in the forward direction for one walking trial. The data collection started with the participant at a standstill and stopped with the participant at a standstill, therefore, the velocity at the beginning and end of the trial should be zero. Figure 3.3 shows the initial velocity to be zero but the final velocity to be close to -4m/s. The discrepancy between zero and negative four in the velocity signal is due to inaccuracies in the original acceleration signal.

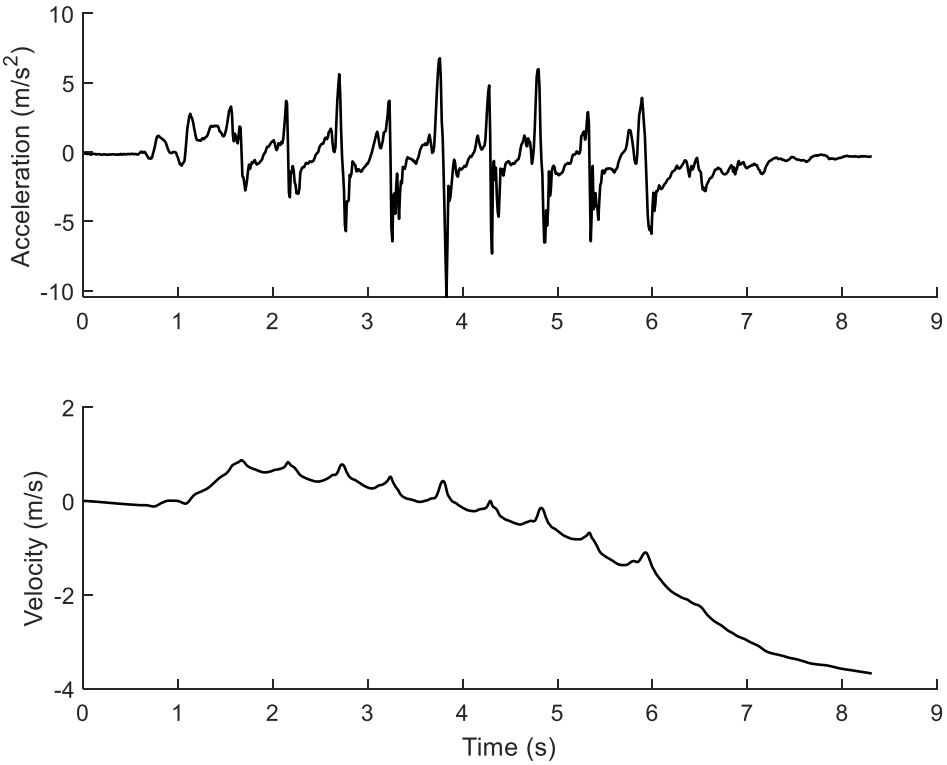

Figure 3.3: The inaccuracy in velocity caused by drift in the acceleration signal when using mathematical integration to calculate velocity from acceleration.

3.3 Optimal Filtering

Filtering the acceleration signal can reduce the amount of drift. A band-pass filter will remove both high frequency and low frequency noise from the signal. A band-pass filter led to a slightly more accurate calculation of velocity from acceleration. But caution must be exercised when analyzing a movement such as gait, as the filter cutoffs must be set to avoid the fundamental frequency of the movement (Zok, Mazzà, & Della Croce, 2004). Optimal filtering has been used in studies that have accurately calculated the velocity and displacement using wearable accelerometer sensors (Köse, Cereatti, & Della Croce, 2012; Zok et al., 2004). The glaring issue in these studies and others was that the optimal cut-off frequencies are determined by comparing the sensor results to result from a motion tracking system. Typically, the accelerometer data is filtered at different frequencies until the researchers find the frequency cut-offs that elicit velocities and displacements most similar to those from the motion capture system. There is no way to achieve similar results without comparison to motion capture data. Figure 3.4 shows a very slight improvement compared to the first method in the calculation of velocity from anterior-posterior acceleration, although there was still inaccuracies in the velocity, the inaccuracies are less than the velocity displayed in Figure 3.3. Removing the linear trend that occurs from the start of the data to the end would further increase the accuracy of the calculated velocity and displacement.

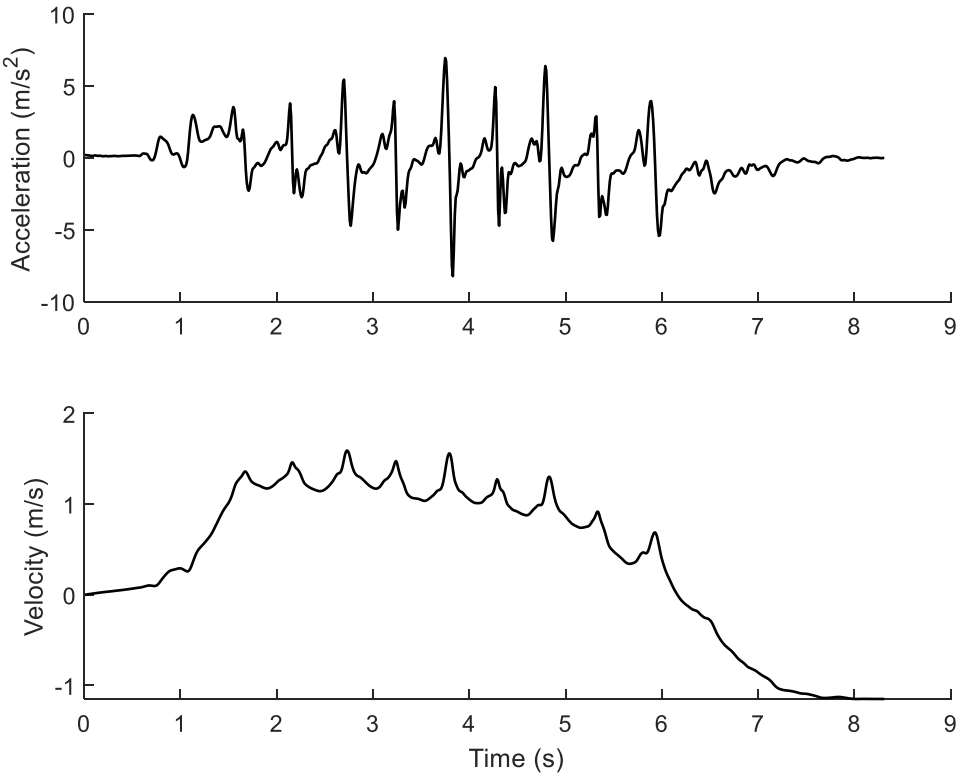

Figure 3.4: The velocity inaccuracy when a band-pass filter (1 Hz & 20 Hz cut-off frequencies) was applied to the acceleration data prior to mathematical integration.

3.3.1 Optimal Filtering and Removal of Linear Trend

Combining the optimal filtering with the removal of the remaining linear drift in the signal further improves the accuracy of the calculated velocity and displacement. Because we know what acceleration and velocity values to expect when the sensor is stationary, these stationary times serve as times where linear trends can be removed from the data (Madgwick, 2014). For example, in Figure 3.4 above, we know that the velocity in the forward direction at the start and the end of the trial should be zero. Because the velocity value at the end of the trial is not zero, we know it has been affected by drift in the acceleration signal. The linear trend that occurs between the two stationary time points (beginning and end of trial) can be calculated and removed (Figure 3.5).

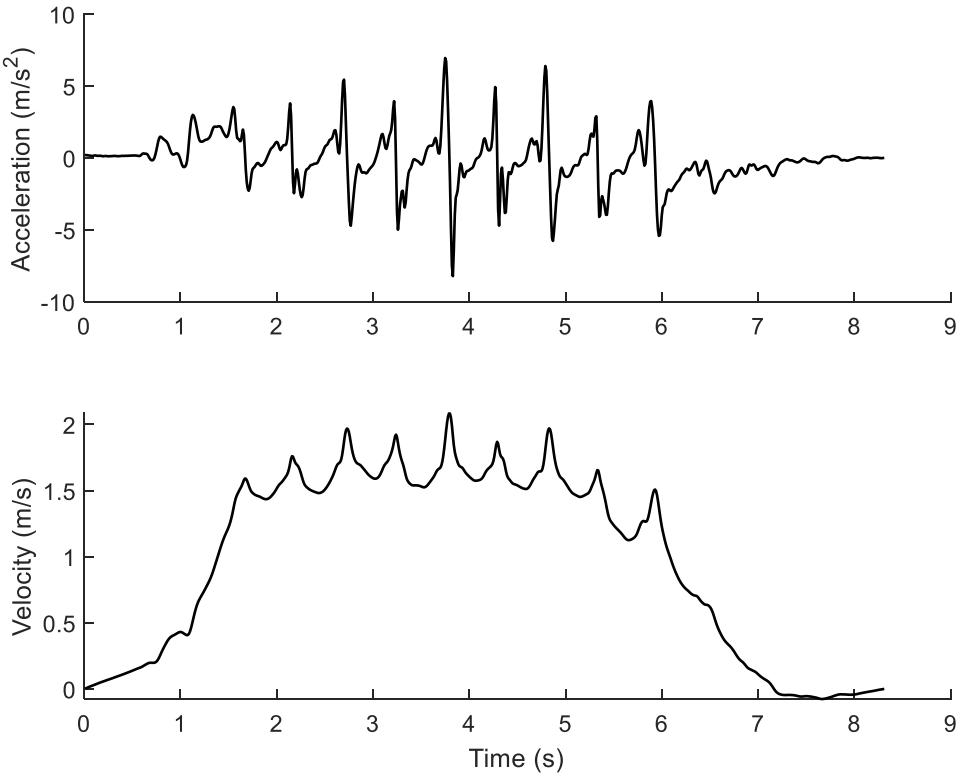

Figure 3.5: Velocity after a band-pass filter (1 Hz & 20 Hz cut-off frequencies) was applied to the acceleration data and the linear drift rate in the resultant velocity data was calculated between the stationary time at the beginning and end of the trial and removed.

3.3.2 Optimal Filtering and Direct-Reverse Integration

A 2004 technical note (Zok et al., 2004) proposed a method of integration to minimize the amount of drift that occurs when integrating a signal. In short, direct-reverse integration (DRI) integrates the signal in both the forward and backwards directions and combines them together using a weighting function. The rationale for this technique is that the errors accumulate as you integrate, so by integrating the acceleration from the beginning you have less error at the start of the resultant velocity and by integrating backwards from the end of the acceleration signal you have less error at the end of the resultant velocity. A weighting function is then used to combine the forward and backwards integrations (Equation 5 & 6). The beta value in Equation 6 controls

the shape of the weighting function and in the technical note a beta value of 0.1 was proposed, but a beta value of 0.4 worked best with the data in the current work.

Equation 5: Direct-Reverse integration formula, combining the forward and backward integration.

$$w(t) = \frac{s(t)-s(t_B)}{s(t_E)-s(t_B)}$$

Where:
$t = time$
$t_B = time\ at\ the\ beginning$
$t_E = time\ at\ end$

Equation 6: The weighting curve for DRI.

$$s(t) = \arctan\left(\frac{1}{\beta}\frac{(2t-t_E)}{2t_E}\right)$$

Where:
$t = time$
$t_E = time\ at\ end$
$\beta = shape\ of\ the\ curve$

Zok et al. (2004) proposed that the direct-reverse integration technique be used with a band-pass filter in order to obtain the optimal results. The problem of choosing filter cut-offs was reiterated in this technique, as motion tracking was used to choose the optimal filter cut-offs so that a velocity that most closely matches the motion capture data could be obtained. Figure 3.6 shows the same forward acceleration data from above being processed using bandpass filtering and direct-reverse integration.

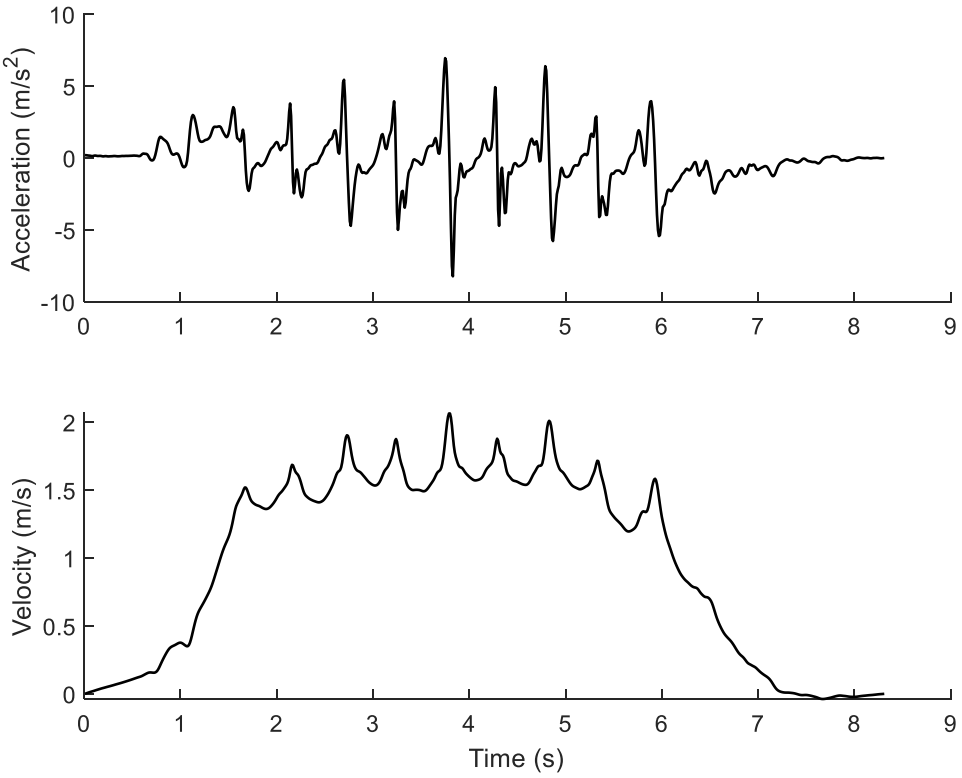

Figure 3.6: Forward velocity calculated band-pass filtering the acceleration data (1 Hz & 20 Hz cut-off frequencies) and direct-reverse integration.

Comparing Figure 3.5 and Figure 3.6, the optimal filtering, and the removal of linear drift technique and the optimal filtering combined with direct-reverse integration yielded very similar results, but they present different ways of handling the linear drift present in the acceleration signal.

The above techniques used the acceleration signal directly to calculate velocity, while employing different techniques to compensate for the linear drift that is present because of artifact in the original acceleration signal. The remaining two techniques to be discussed are signal reconstruction techniques: principle component analysis (PCA) signal reconstruction and Fourier-based signal reconstruction.

3.3.3 Principle Component Analysis Signal Reconstruction

Principle component analysis (PCA) aims to reduce the dimensionality of a dataset that has many related variables (Jolliffe, 2002). This reduction is achieved by creating new variables based on the covariance in the original dataset (Abdi & Williams, 2010; Smith, 2006). After performing a PCA on a signal, a new dataset, expressing the original data in terms of the components is created, as well as many eigenvectors and eigenvalues, which are dependent on the data structure. The eigenvectors represent the variance in the data while the eigenvalues are weightings for each corresponding eigenvector. The first eigenvector represents the most variation, with a decreasing amount of variance represented by the latter eigenvectors (Smith, 2006). The original data can be reconstructed from the transformed data using the eigenvectors. To reconstruct the original data fully, one would use all eigenvectors (Equation 7). However, not all eigenvectors have to be used. By retaining only, the first few eigenvectors one can selectively reduce the variation in the reconstructed signal.

Equation 7: Principal Component Analysis reconstruction formula.

$$Xpca = (score * \lambda') + \bar{x}$$

Where:
$Xpca = Reconstructed\ signal$
$score =\ the\ original\ data\ represented\ in\ the\ component\ space$
$\lambda =\ the\ eigenvector\ matrix$
$\bar{x} = mean\ of\ original\ data\ set$

Note: Score and eigenvector variables are *m* x *n* matrices, where *n* is equal to the number of components used to reconstruct the signal

With respect to the sensor data in the current work, we wished to remove variance from the data that was caused by factors such as movement artifact or drift. Removing unwanted variance in the data is achieved by omitting components that cause small amounts of variation, then reversing the PCA to reconstruct the original signal (with some variance removed). The first few components represent the greatest variation in the original dataset and likely contain the information from the

original signal that is caused by the 'real movement'. Principle component analysis reconstruction technique yields good results when reconstructing acceleration data for a single stride (Figure 3.7).

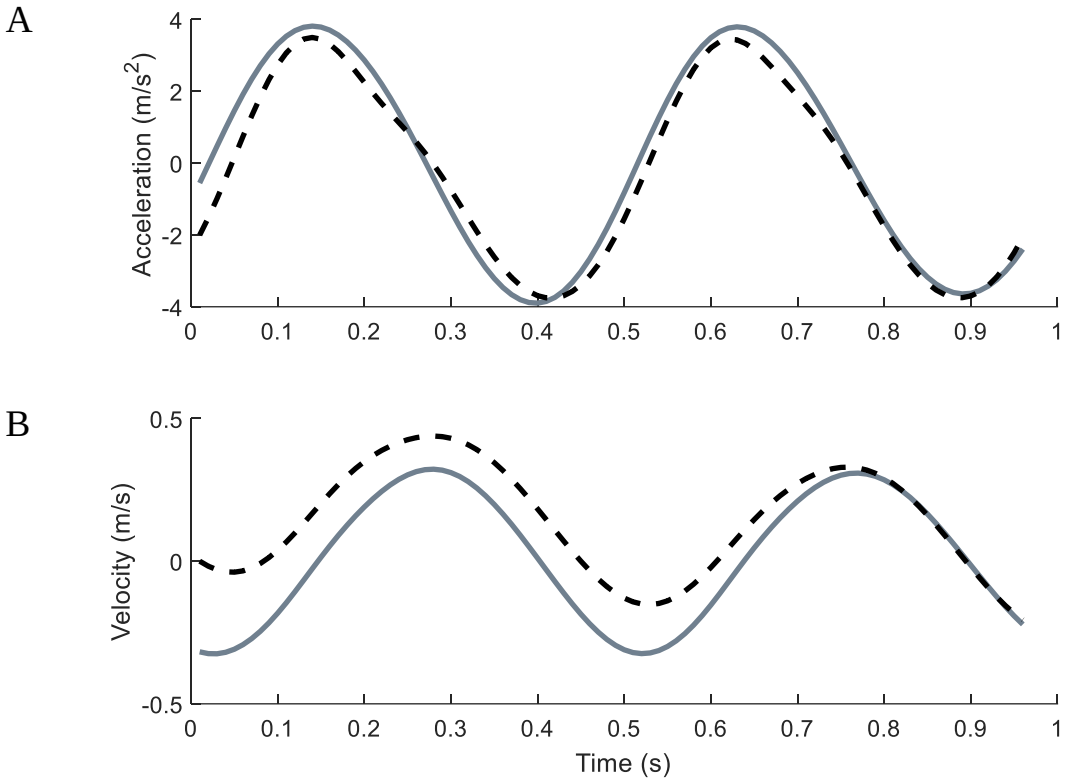

Figure 3.7: A: Comparing PCA reconstructed vertical acceleration from the low back sensor for a single stride (black dashed line) to low back acceleration during a single stride calculated from motion capture data (grey solid line). **B:** Comparing vertical velocity calculated by mathematically integrating the PCA reconstructed vertical acceleration from the low back sensor for a single stride (black dashed line) to low back vertical velocity during a single stride calculated from motion capture data (grey solid line).

3.3.4 Fourier Based Signal Reconstruction and Integration.

A fast-Fourier transform (fft) is a process where a signal is broken down into its harmonic parts. The fft outputs the signal in the frequency spectrum. Each frequency has a power value that represents that specific frequency's contribution to the original signal. A frequency with higher power is more prominent in the signal.

Two methods of Fourier based processing were explored: (1) preforming an fft of the acceleration signal, zeroing out the harmonics below a certain power threshold and reconstructing the signal using an inverse-Fourier transform, (2) calculating the coefficients for cosine and sine respectively and performing Fourier based reconstruction and integration.

The first of the two techniques is the simplest and is similar to filtering the acceleration data, in that it removes frequencies that are less important to the shape of the original data. This technique is different than traditional filtering because the frequencies that are removed from the signal are selected based on their power, and not just frequency thresholds. Figure 3.8 shows the original acceleration signal and the reconstructed signal after zeroing out the frequencies with low power amplitudes. From the reconstructed signal mathematical integration can be performed to yield the velocity and displacement values.

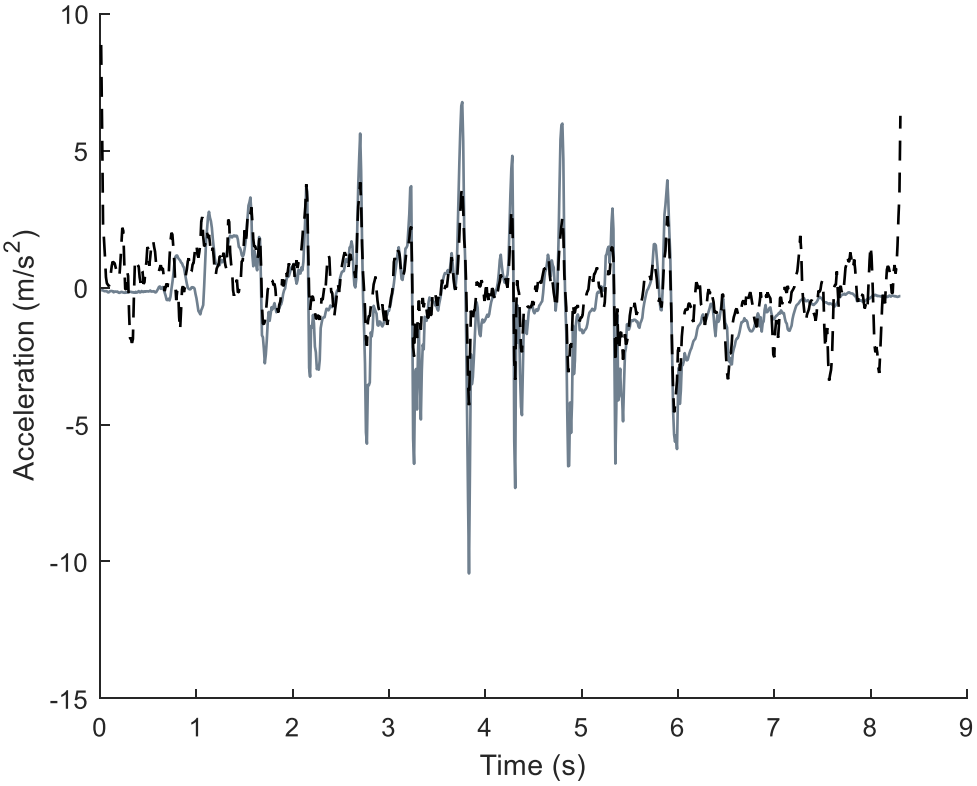

Figure 3.8: Reconstructed acceleration signal (dashed line) compared to the original signal (solid line), after preforming an fft and zeroing out frequencies with amplitudes less than 5 m/s^2.

The second of the two Fourier processing techniques involved splitting the acceleration profile of one walking trial into strides and performing Fourier reconstruction and analytical integration for each stride individually. Analytical integration avoids the effects of drift in the signal as the integration that is performed is based on the identified trigonometric polynomials found to be components within the signal (Sabatini, Ligorio, & Mannini, 2015). To complete this analysis, stride cycles must be identified to guarantee that the analytical integration is being performed on full cycles (a curve that starts and ends at the same point on the y-axis), and not fractions of a cycle. The reason full cycles are required is because the signal is reconstructed using cycles of the sine

and cosine waves. If this technique were used on an incomplete cycle the accuracy of the reconstructed signal would be compromised as the reconstructed curve would reflect a full cycle even though it should not, making the final values of the reconstructed signal incorrect. From an accelerometer attached to the lower back, heel contacts can be identified by the peak anterior-posterior acceleration (Figure 4.7; Zijlstra, 2004). Once heel strikes are identified the acceleration signal is split into complete stride cycles. To calculate the Fourier coefficients for reconstruction and integration to take place, there are two options. MATLAB's 'fit tool' reconstructs the signal based on a maximum of eight Fourier coefficients. This yields less accurate results than using more than eight coefficients. Twenty Fourier coefficients were used by Sabitini and colleagues (2015) in their gait study to reconstruct a signal and integrate to velocity and displacement. If more than eight coefficients are required, they can be calculated from an fft where the real part of the fft can be used to calculate the coefficients for the cosine series and the imaginary component of the fft corresponds with the sine series. The analytical integration is performed using the following equations:

Equation 8: Acceleration reconstruction formula.

$$acc_i = \sum_{k=1}^{N} \left(a_i(k) \cos \frac{2\pi k}{T_i} t + b_i(k) \sin \frac{2\pi k}{T_i}\ t \right)$$

Equation 9: Velocity reconstruction formula.

$$vel_i = \frac{T_i}{2\pi} \sum_{k=1}^{N} \frac{1}{k} \left(a_i(k) \sin \frac{2\pi k}{T_i} t + b_i(k) \cos \frac{2\pi k}{T_i}\ t \right)$$

Equation 10: Displacement reconstruction formula.

$$disp_i = \left(\frac{T_i}{2\pi} \right)^2 \sum_{k=1}^{N} \frac{1}{k^2} \left(a_i(k) \cos \frac{2\pi k}{T_i} t + b_i(k) \sin \frac{2\pi k}{T_i}\ t \right)$$

Where:
$i = stride\ number$
$N = number\ of\ harmonic\ coefficients$
$T = total\ length\ of\ stride\ cycle$
$t = time\ step$
$a = coefficients\ from\ the\ real\ component\ of\ the\ fft$
$b = coefficients\ rom\ the\ imaginary\ component\ of\ the\ fft$

Coefficients ‘a’ and ‘b’ in the above equations can be calculated using the equations below (Storey, n.d.). The maximum number of coefficients that can be calculated is equal to half of the length of the original signal. An example of the resulting signal reconstruction and integration to velocity and displacement data can be found in Appendix A (pg. 79).

Equation 11: Formula to calculate cosine series coefficients.

$$a = \frac{2}{N} * real$$

Equation 12: Formula to calculate sine series coefficients.

$$b = -\frac{2}{N} * imaginary$$

Where:
$N = number\ of\ data\ points\ in\ the\ original\ signal$
$real =\ the\ real\ component\ of\ the\ fft$
$imaginary =\ the\ imaginary\ component\ of\ the\ fft$

3.4 Head and Low Back Sensors Collecting Out-of-Sync

It is of utmost importance with respect to the current work that the data from the low back and head sensor be collected in sync with one another. The reason synchronization is required is that the algorithms used to partition the data into strides are based on the low back accelerations. If the two sensors are not in sync, then the head sensor data will be partitioned at the wrong time points.

Any synchronization problems can be resolved because the vertical acceleration of the low back and the vertical acceleration head are tightly coupled and occur at the same time, therefore the lag between the head an low back data can be calculated by aligning the head and low back vertical accelerations. Once the lag is calculated, it can be used to synchronize the head and low back acceleration signals in time.

3.5 Conclusion

There is no perfect solution to calculate velocity and displacement data from an accelerometer. It is possible to get accurate results using filtering, but the cut-off frequencies need to be chosen by comparison to a gold standard. The Fourier reconstruction and analytical integration of the signals is the only method that was identified that does not compare to motion capture data to select optimal filter cut-off frequencies. Although, the results may be slightly less accurate, this seems like a good

option when using accelerometers outside of the lab, as comparison to motion capture data is not be available.

A method of selecting the optimal frequency cut-offs without comparing to motion capture data would be ideal, and further strengthen the use of accelerometers in the clinical setting. But no such method currently exists.

Chapter 4

Methodology

4.1 Participants

Fifteen healthy-young adults were recruited to participate in this study (age: 25.2 years ± 2.1 years, mass: 67.8kg ± 6.7kg, height: 1.7m ± 0.07m). Their height, injury history and limb dominance were recorded. The inclusion criteria for this study were healthy adults between the ages of 18-30. Queen's University General Research Ethics Board approved the protocol (Appendix B; pg. 83) and all participants gave written, informed consent before participating.

4.2 Setup

Before beginning data collection, the motion capture system was calibrated. Only calibrations with an error (measured by the standard deviation of marker location during calibration) of less than 0.5 mm were accepted as adequate calibration of the system. If the 0.5 mm threshold was not met, the calibration was redone.

4.3 Experimental Conditions

The five experimental conditions were: A control condition, where the participant completed the protocol in their own shoes, a zero AFO condition where the participant was outfitted with the orthotic on their right side but no heel wedges or restrictions were added, and three conditions where the participant wore the orthotic with low, medium or high heel wedge inserts all with restricted dorsiflexion. Before each condition was collected, participants practiced walking with the AFO. Data collection did not start until the participant gave verbal acknowledgment that they were comfortable walking with the orthotic and heel lift. The order of the conditions was randomized for all participants. Each condition consisted of ten walking trials. A trial was defined as walking one length of the laboratory (approximately 7 meters; Figure 4.1).

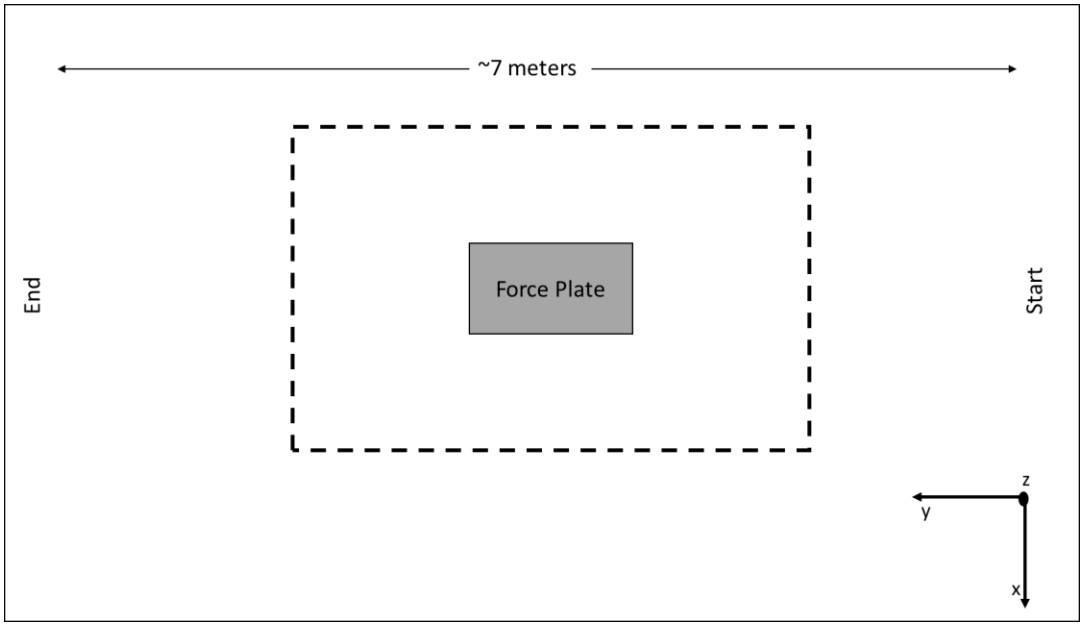

Figure 4.1: Overhead diagram of the lab space. The approximate field of view of the motion capture cameras where motion capture data was collected is identified by the black dashed line surrounding the force plate. The lab coordinate system is defined in the bottom right corner, with the direction of progression along the y axis.

4.4 Ankle-Foot Orthotic (AFO) and Heel Wedges

To accommodate participants of different foot sizes, two ankle-foot orthotics (Figure 4.2) were made. The smaller of the two orthotics could accommodate individuals with men's shoe sizes between six and ten. The larger of the two orthotics could accommodate individuals with men's shoe sizes between ten and thirteen. Participants wore the orthotic on their right foot. All participants were fitted with the orthotic that best matched their foot size. Participants wore a high-top Converse shoe on their right side (AFO side) during the AFO conditions and their own shoe on their left foot (participants were told to wear a shoe that they considered to be suitable for walking). The Converse shoe was chosen because its sole is relatively flat. The tongue of the shoe was cut off (Figure 4.3) so that markers could be placed directly on the foot segment (one on the midline of the foot over the tarsals, and one over the metatarsals), and the laces were replaced with hockey

laces in order to accommodate the added volume of the heel wedges in the shoe (under the orthotic) during the medium and high wedge conditions.

Figure 4.2: One of the ankle-foot orthotics used in the study. The strap to limit dorsi-flexion (located on the back of the orthotic) during gait is circled. The strap was tightened before the start of each experimental condition.

The heel wedges were fabricated out of a high-density foam. Five individual, stackable wedges were used (Figure 4.4). Each individual heel wedge increased plantar-flexion angle by approximately 5 degrees. The small wedge condition used a single heel wedge, creating approximately 5 degrees of plantar flexion. The medium wedge condition used three wedges, creating approximately 15 degrees of plantar flexion. The high wedge condition used all five wedges and created approximately 25 degrees of plantar flexion.

The strap at the back of the AFO (Figure 4.2) was used to restrict dorsiflexion during the swing phase. The strap was the last adjustment made to the AFO before beginning a trial because the heel wedges needed to be in place before tightening the strap to the appropriate length. To tighten the strap, the participant was instructed to stand with their knee in full extension on the AFO side, the strap was then tightened as much as possible. The dorsiflexion restrictive strap was used in the low, medium and high wedge conditions, but not the zero AFO condition.

Figure 4.3: Converse shoe with the tongue removed to accommodate marker placement directly on the foot.

A

B

Figure 4.4: A: The five heel wedges stacked together, creating the maximum heel lift possible. Wedges were stuck together using double-sided tape. **B:** The five wedges separated; each wedge creates approximately five degrees of plantar flexion. The wedges were added into the shoe, underneath the ankle-foot orthotic.

4.5 Equipment

Before testing, eighteen 14 mm reflective tracking markers were placed at specific anatomical landmarks on the participant (Figure 4.5 & Figure 4.6). A thirteen camera Qualisys Motion Tracking System (Qualisys Track Manager, Qualisys, Gothenburg, Sweden) sampling at 100 Hz tracked these reflective markers during data collection. In addition, two inertial measurement units (IMU; mbientlab, metamotion-r3, San Francisco CA) were attached, one to the head and the other to the low back (as an estimate of CoM location; Figure 4.5 & Figure 4.6). The IMUs recorded linear acceleration and the dynamic gravity vector at 100 Hz and the data was stored onboard the

IMUs during each experimental condition and downloaded upon its completion. The IMUs were then reset to start a new collection for the next experimental condition.

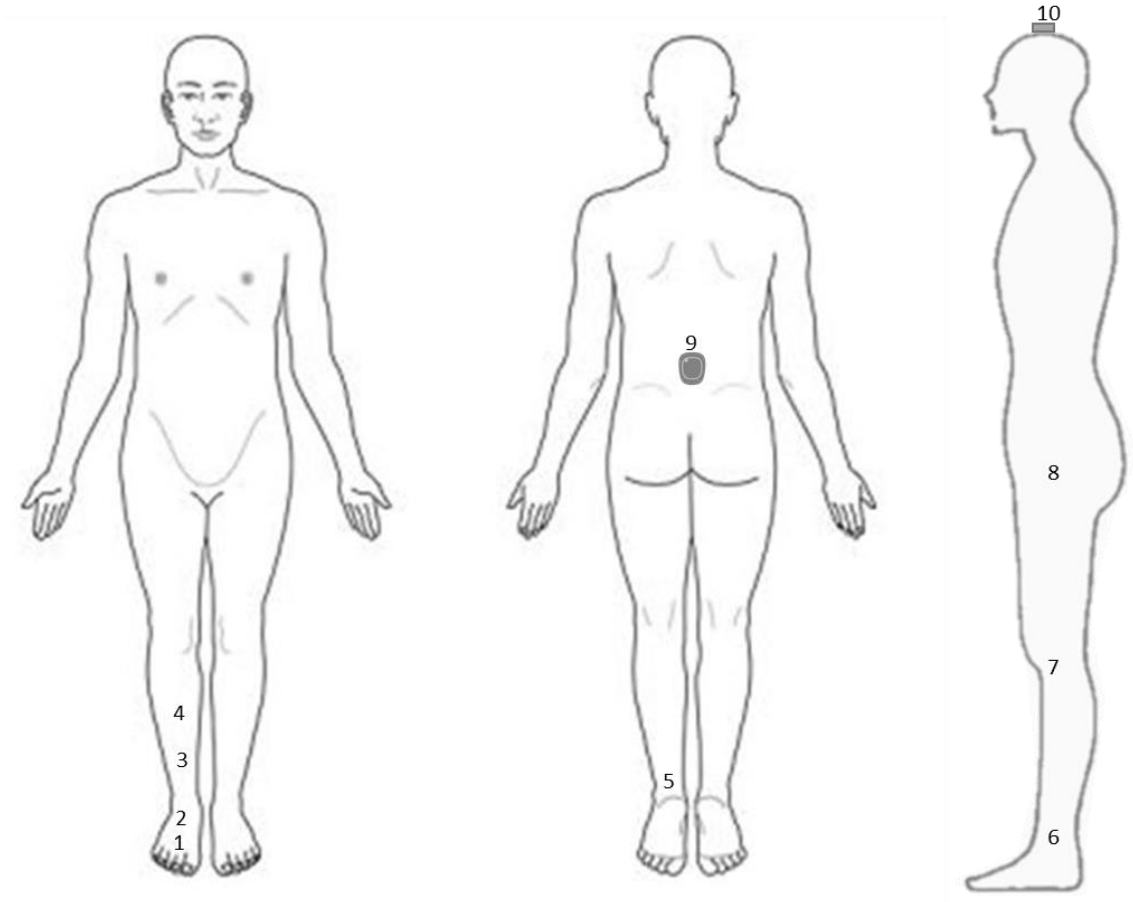

1	Defines the distal end of foot segment (midline of the foot, over the tarsals)	8	Greater trochanter
2	Defines the proximal end of the foot segment (midline of the foot over the metatarsals)	9	Low back sensor/marker
3	Defines the distal end of foot segment	10	Head sensor/marker
4	Defines the proximal end of the foot segment		
5	Left heel		
6	Lateral malleolus		
7	Lateral femoral condyle		

Figure 4.5: Marker and sensor placement. Markers 1-8 were place bilaterally.

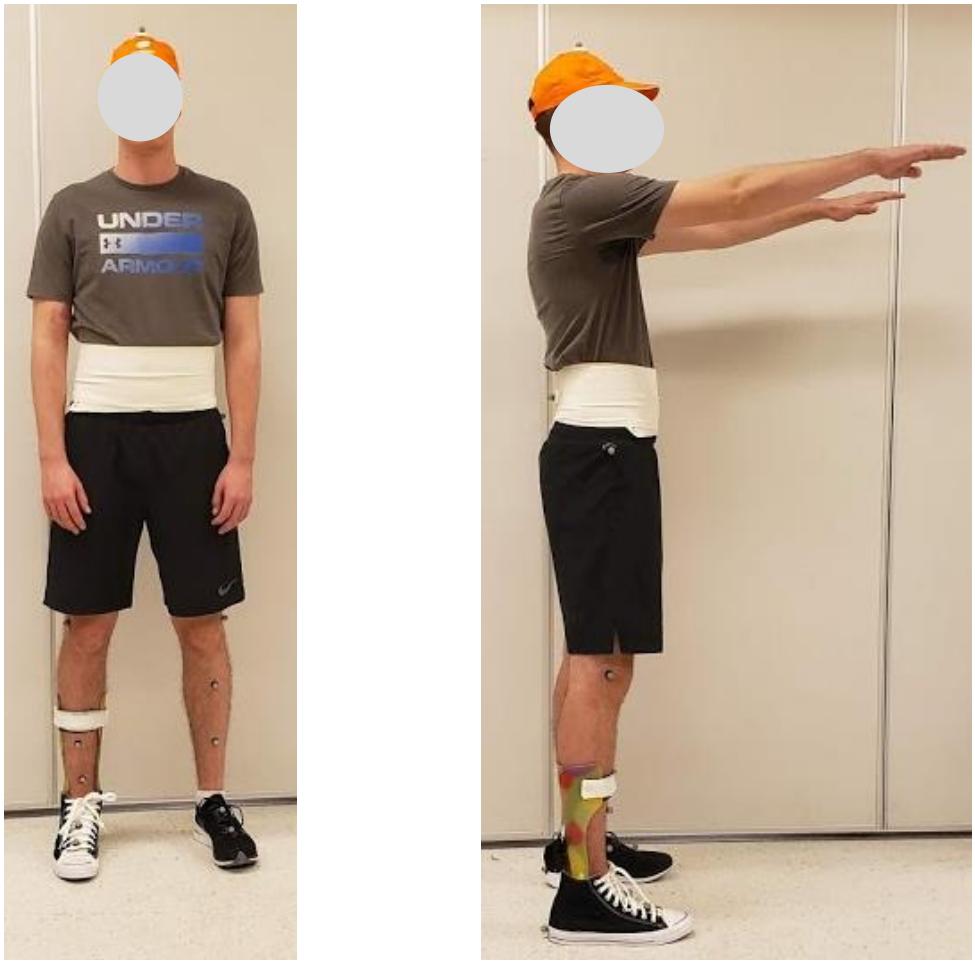

Figure 4.6: Participant instrumented with markers and sensors.

4.6 Data Collection

4.6.1 Protocol

Before the start of the data collection the participant was told of the verbal cues that would be used to instruct them during the data collection. The participant was told to ‘start’, ‘pause’ and ‘turn’ at different times throughout the collection. The ‘pause’ instruction was used to ensure that there was enough quiet standing at the end of each trial, so that the IMU data could be easily separated into trials. The instruction to ‘turn’ was used after the pause, to instruct the participant to turn and prepare to walk back in the other direction. Participants performed all trials at a comfortable walking pace.

A static trial was collected before each experimental condition, during which the participant was stood still in the middle of the lab for five seconds. This allowed static marker and sensor measurements to be recorded. During the static trial, a goniometer was used to measure the ankle angle of the AFO leg.

At the start of each condition the participant assumed a quiet standing position at one end of the lab. On the researcher's cue the participant walked the length of the lab and stopped at the other end. There was then a pause of approximately two seconds, then the participant turned and prepared to walk back in the other direction. A trial was defined as a walk of one length of the laboratory (Figure 4.1). After the ten trials were complete there was a break of approximately 5 minutes. During this time, if needed, the heel wedges were adjusted for the next condition, and the participant completed a five question Qualtrics survey (Appendix C, page 85). The survey was administered on an iPad Mini (screen diagonal: 20.1 cm). All questions were answered using a slider response system. The survey contained questions relating to their perception of stability and effort throughout the walking trials.

4.7 Data Analysis

Preliminary analysis of the marker data was done in Qualisys Track Manager. The data were then exported to MATLAB 2019a for further processing and calculation of the outcome variables. IMU data were downloaded from the sensors as CSV files. These files were read directly into MATLAB 2019a for processing. Finally, statistical analysis was performed using SPSS.

4.7.1 Qualisys Track Manager

Upon the conclusion of the data collection, markers were labelled by location (Figure 4.5) and gaps in marker tracking of less than 20 frames were filled using Qualisys' polynomial fill function, which fits a third order polynomial to the missing data. Since the walking trial began and ended with the participant out of the collection frame (Figure 4.1), the marker data was clipped such that the markers on the two IMUs (markers 9 & 10; low back & head) were recorded by the motion

tracking system 100% of the time. This allowed for at least one full stride of the left and the right legs to be captured within the collection space. Markers 1-8 (Figure 4.5) were included as part of the setup in anticipation of completing a joint angle analysis. But since the trials were clipped to optimize the tracking of the low back and head markers, and the other markers were often missing from the frame, we chose to only analyze the low back and head marker data. After this preliminary processing, the data were exported to MATLAB 2019a.

4.7.2 MATLAB 2019a

Custom MATLAB code was written to further process the marker data and process the acceleration and gravity data from the IMUs.

4.7.2.1 Marker Data

First, the mean vertical and mediolateral position of the marker placed on the low back sensor and the marker placed on the head sensor were subtracted from their respective displacement data to detrend the data, allowing it to be more easily compared to the accelerometer data from the IMUs. Next, the marker data was differentiated to calculate velocity and then again to calculate acceleration. A dual pass butterworth filter with a frequency cut-off of 20 Hertz was used after each differentiation. Once the velocity and acceleration had been calculated, the acceleration data of the low back IMU marker was used to identify heel strikes, which in turn was used to identify stride cycles. Heel strikes were identified by the peak anterior-posterior acceleration of the marker attached the low back IMU (Figure 4.7; Zijlstra, 2004). Once heel strikes were identified, strides, the time between successive heel strikes, were identified. The mediolateral displacement of the low back marker was used to identify whether a stride started with a left or right heel strike. If the first peak of the mediolateral displacement of the low back marker was positive the stride was a left foot stride, and if the first peak was negative the stride was a right foot stride. The low back and head marker data were separated into strides and sorted into left or right strides according to the heel strike, and mediolateral displacement position data from the low back marker.

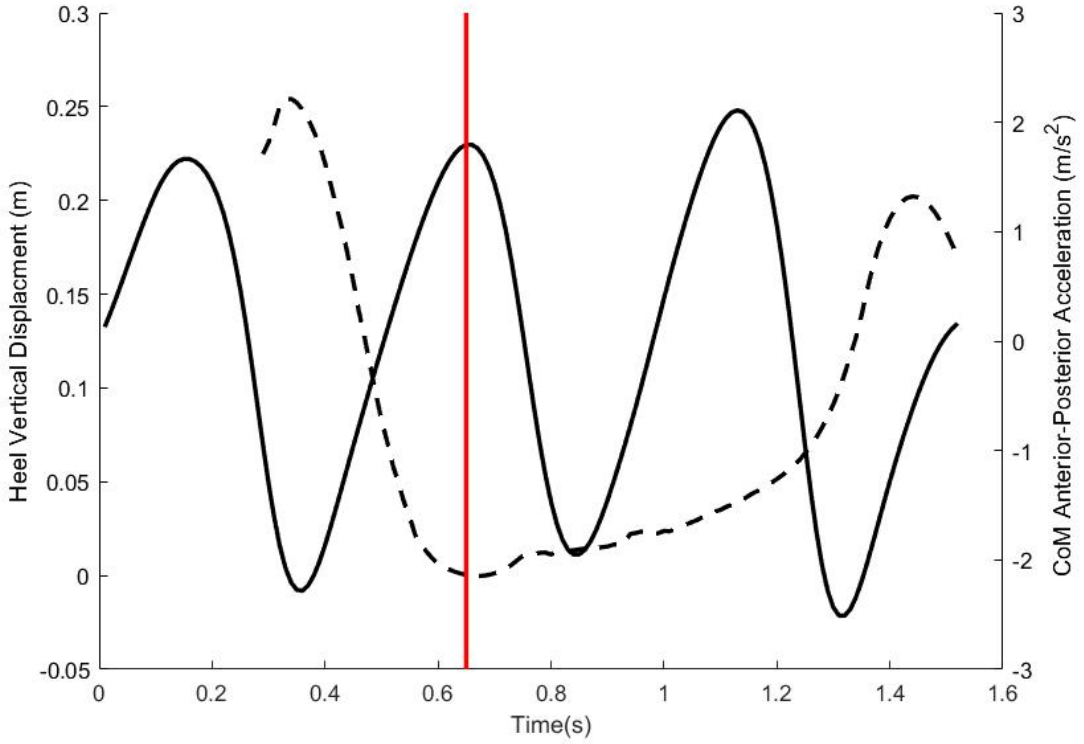

Figure 4.7: Anterior-posterior acceleration (black solid line) is plotted with the vertical displacement of the right heel marker (black dashed line). The instant of heel strike is shown by the red vertical line. The peak anterior-posterior acceleration is in line with the heel's minimum vertical displacement, providing evidence that peak anterior-posterior acceleration is a valid way of identifying heel strikes during walking.

With the marker displacement, velocity, and acceleration data separated into strides and sorted by which side the stride began on, the marker data was used to calculate the outcome variables of interest. The acceleration, velocity and displacement data of all strides that started with a right footed heel strike were averaged for each individual participant, yielding average right-stride data on each axis of motion. Outcome variables were calculated for each individual participant using the mean stride data.

4.7.2.2 IMU Data

The IMU data were collected continuously for each experimental condition, in other words the IMU collection was not stopped between trials, it collected data continuously from the start of trial one to the end of trial ten for one experimental condition. The method of continuous collection was selected to make data collection more efficient, as it took three to five minutes to stop and download the data from the IMUs. Since the IMU data for the ten walking trials of each condition was collected continuously the data first had to be separated into trials. The net acceleration (the square root of the sum of the squares of the X, Y and Z accelerations) was calculated to determine when the IMU was stationary at the beginning and end of each walking trial (Madgwick, 2014). The accelerometer was considered stationary when the net acceleration was less than 0.85 m/s^2. The threshold was chosen after a visual inspection of the net acceleration data and was the same for all participants. After the acceleration data was separated into individual trials, the data of both the low back and the head for each walking trial were detrended to remove any offset and lowpass filtered with a cut-off of 25 Hz.

Next, the acceleration data was corrected for sensor tilt (Figure 4.8). An accelerometer attached to the lower back at the approximate location of the body's CoM is known to be tilted because of the natural curve of the lower back (Meichtry, Romkes, Gobelet, Brunner, & Müller, 2007). The IMUs (mbientlab, metamotion-r3, San Francisco CA) can separate linear accelerations (accelerations caused by motion) from the gravity vector (gravitational accelerations). The onboard processing to separate linear acceleration and gravitational acceleration makes use of the other sensors built into the IMU such as the magnetometer and the gyroscope. To correct for the orientation of the IMU and rotate the IMU axes to match the lab coordinate system, the gravity vector output from the sensors was used. Using the gravity vector from each IMU, a simple vector rotation was performed to correct for the orientation of the sensor. First, the rotation angle required to rotate the gravity vector back to one g (acceleration due to gravity) on the vertical axis [0 0 1] was calculated for each time point in the gravity data. Then, that rotation was applied to the linear

acceleration data, which aligned the orientation of the sensor data with the lab's coordinate system. After the orientation correction, the acceleration data was separated into strides using the peak antero-posterior acceleration of the low back.

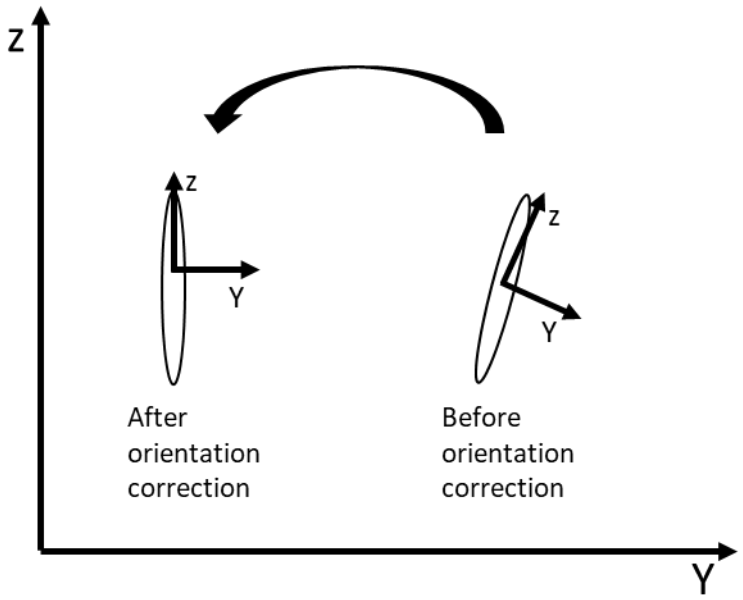

Figure 4.8: Diagram of sensor orientation correction. The lab coordinate system is represented by the large outer axes, and the local sensor coordinate system is represented by the smaller axes. Before the orientation correction was applied forward and vertical acceleration data could not be considered mutually exclusive entities. The rotation necessary for correction was calculated using the gravity vector. For example, in the figure before the correction is applied there is 0.3g on the y axis and 0.7g on the z axis. The correction is the rotation necessary to achieve 1g on the z axis and 0g on the y axis.

Though this orientation correction was simple and easy to apply, it had one major limitation, which was it was not sensitive to rotations about the gravity axis. In other words, we could not correct for a misalignment of rotation about the vertical axis. Therefore, we ensured that all participants completed their walking trials while looking straight ahead. Furthermore, since the walking was completed at a comfortable walking pace and the low back IMU was positioned in the

centrally, we assumed that the change in orientation of the low back IMU about the vertical axis was negligible.

Once the acceleration data was separated into individual strides the Fourier-based integration technique (Chapter 3) was used to calculate the velocity and displacement data of both the head and low back IMUs. Finally, the mediolateral displacement data, calculated from the low back IMU mediolateral acceleration, was used to sort the strides by left and right sides (defined by which foot the stride began with). The acceleration, velocity and displacement data of all strides that started with a right footed heel strike were averaged for each participant, yielding average right-stride data for each axis of motion. All outcome variables were calculated for each individual participant using the mean stride data.

4.8 Outcome Variables

There were four outcome variables, two measures of gait efficiency and two measures of stability. All four-outcome variable were calculated twice, once using the sensor data and once using the marker data. Ensemble averages of each outcome variable were calculated by averaging the results of all trials for each participant. The outcome variables calculated from the IMU sensors were compared to the outcome variable calculated from the marker data to verify the concurrent validity of the sensors. Concurrent validity is a type of criterion validity that compares a new measure or system to a benchmark to assess how similar they are.

Due to a collection issue with one of the IMU sensors, data from one participant had to be excluded. Therefore, all outcome variables were calculated with the data from fourteen participants (N = 14). Background information, of the variables was provided in the review of literature (Chapter 2). The following paragraphs will outline more clearly how the variables were calculated from the data collected.

4.8.1 Biomechanical Efficiency Quotient (BEQ)

The BEQ is a ratio of predicted vertical excursion of the CoM to the actual vertical excursion of the CoM (estimate from the low back sensor and marker) during a walking stride. Equation 4 is used to predict the COM's vertical excursion and the actual excursion is from the sensor or marker data. For the sensor data the CoM vertical excursion was calculated from the IMU accelerations by double integrating the acceleration signal using the Fourier-based integration technique. For the marker data the low back vertical excursion was tracked using the marker attached to the low back IMU. The quotient is calculated by dividing the measured vertical excursion by the predicted excursion. This project used leg length as an approximation of sacral height. Leg length was the vertical distance between the left heel marker and the left greater trochanter marker during a static trial. If the BEQ were used in clinic, leg length could be measured manually or estimated from anthropometric tables. For the marker data stride length data was measured from the low back marker. For the sensor data, stride length was calculated by dividing the known distance walked by the number of steps taken and multiplying by two (Menz et al., 2003b). The BEQ was calculated for each participant from the mean vertical excursion of the low back marker/sensor and the mean stride length for each experimental condition.

Equation 4: Vertical CoM excursion prediction equation

$$p = \frac{1}{2}(h - \sqrt{h^2 - \left(\frac{1}{4}l\right)^2})$$

Where:
p *is the predicted vertical center of mass excursion*
h *is the sacral height*
l *is the average stride length*

Note: This equation is copied from Chapter 2 (pg. 16) for reference.

4.8.2 Cross-Correlation of Low Back Anteroposterior Velocity and Vertical Displacement

Cross-correlation is a measure of likeness between two curves. The values range from negative one to positive one where a value of positive one represents two curves that are perfectly in-phase and value of negative one represents two curves that are perfectly out of phase. The cross-correlation between forward velocity and vertical displacement of the low back marker/sensor was used as a measure of gait efficiency. We expect more efficient gaits to produce correlations closer to negative one and less efficient gait patterns to produce values trending in the positive direction.

4.8.3 Harmonic Ratio

The harmonic ratio is a measure of gait stability calculated using the results from a finite Fourier transform. The acceleration data for a single stride was broken into its harmonic parts and the frequencies were normalized to the second harmonic (N = 2). The second harmonic is the fundamental frequency in the anterior-posterior and vertical directions, defined as the frequency with the highest power from the finite Fourier transform. The first 20 frequencies were used to calculate the harmonic ratio (Figure 4.9). In the anteroposterior and vertical directions, gait is biphasic, and the acceleration pattern repeats within a given stride. Therefore, in these directions the signal should be dominated by the even numbered harmonics. The harmonic ratio is calculated by dividing the sum of the amplitudes of the even numbered harmonics (N = 2,4,6…) by the sum of the amplitudes of the odd harmonics (N = 1,3,5…). Since the acceleration patterns in the mediolateral direction are monophasic and only happen once per stride, the signal is dominated by the odd numbered harmonics and the ratio is calculated by dividing the sum of the amplitudes of the odd numbered harmonics (N = 1,3,5…) by the sum of the amplitudes of the even harmonics (N = 2,4,6…). The harmonic ratio was calculated for the mean stride of each condition for each participant, on all three axes (one harmonic ratio for each axis) at both the low back and the head independently. The harmonic ratio scores were then averaged across all participants to obtain one ensemble average of the harmonic ratio values for each axis, for all five conditions.

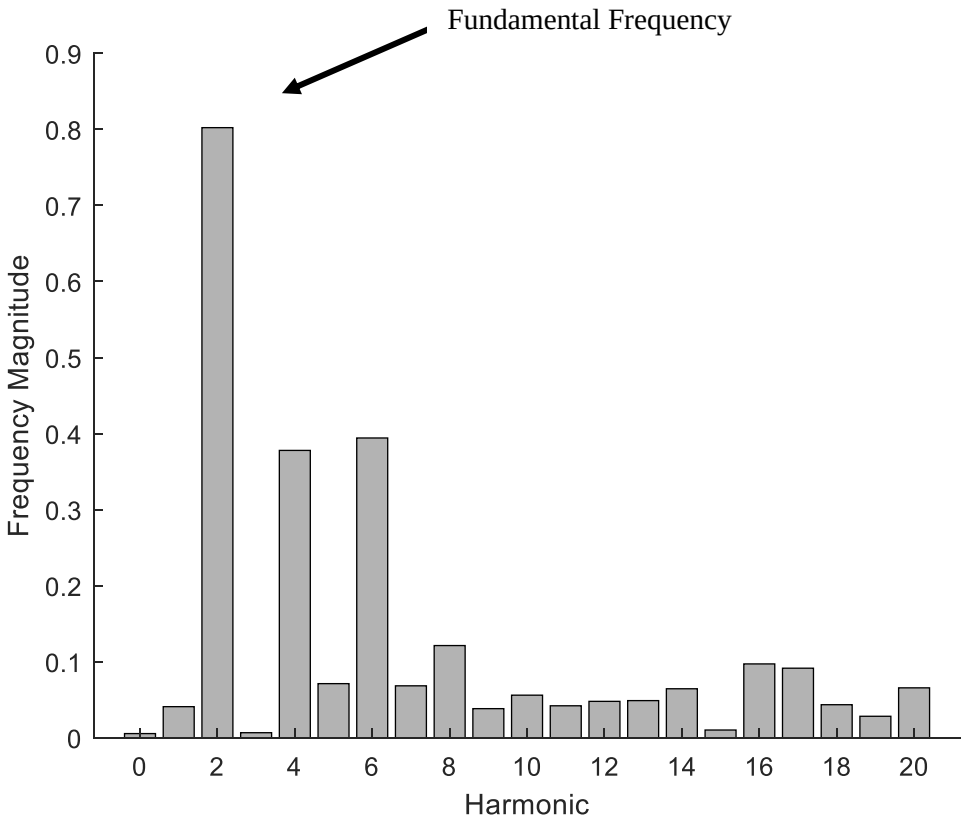

Figure 4.9: A stride's vertical acceleration plotted in the frequency spectrum. The first 20 frequencies in the signal are plotted and the fundamental frequency is identified (N = 2). The harmonic ratio can be calculated from these values.

4.8.4 Acceleration Attenuation from Low Back to Head

The root-mean-square (RMS) of a signal is a measure of signal amplitude. RMS is calculated by squaring the data, calculating the mean, and taking the square root (Equation 13). The RMS of the head and low back accelerations were calculated for all strides in all three direction during all trials after which an average for each experimental condition was calculated. The percent attention

was computed by subtracting the head RMS from the low back RMS then dividing by the low back RMS (Equation 14).

Equation 13: RMS equation

$$acc_{RMS} = \sqrt{\frac{1}{n}\sum_{i=1}^{n} acc_i^2}$$

Where:
$acc = acceleration$
$n = number\ of\ data\ points$

Equation 14: Percent attenuation equation

$$\%\ attenuation = \frac{CoM_{RMS} - Head_{RMS}}{CoM_{RMS}} \cdot 100$$

4.9 Survey Data

Scores for each question were normalized to 100 and averaged across participants for each condition. The survey was to provide some insight on whether the participants were feeling changes in stability and or efficiency when wearing the AFO and heel wedges.

4.10 Statistical Analysis

SPSS (SPSS Inc, Chigaco, IL, USA) was used to complete a statistical analysis of the outcome variables. Repeated measures MANOVAs were used to determine whether there were differences between measurement tools (motion capture vs. sensor), and between experimental conditions. MANOVAs were the statistical test of choice because they maximized statistical power. Significant main effects ($P < 0.05$) were followed up with Bonferroni-adjusted post-hoc comparisons. The absence of a significant interaction effect between measurement tool and experimental condition was interpreted as evidence that the motion capture system and IMU sensors measured similar trends in the outcome variables.

Chapter 5

Results

5.1 Descriptive Statistics of Ankle Angle on AFO Side

Expected plantar flexion angles caused by the heel wedges were: 5 degrees in the low wedge condition, 15 degrees in the medium wedge condition and 25 degrees in the high wedge condition. Table 5.1 displays the average plantar flexion angle across participants.

Table 5.1: Mean plantar flexion angle (degrees) on the AFO side.

	Control mean (S.D.)	Zero AFO mean (S.D.)	Low wedge mean (S.D.)	Medium wedge mean (S.D.)	High wedge mean (S.D.)
Mean	5.2 (3.5)	3.4 (1.5)	10.3 (4.6)	17.3 (5.0)	27.1 (2.9)

Note: Measurements were taken using a goniometer during the static trial (quiet standing; N =15).

5.2 Efficiency Measures

The cross-correlation between forward velocity and vertical displacement of the CoM is a measure of overall gait efficiency and cross-correlation values that are closer to zero, or positive, reflect a less efficient gait pattern. Note that as plantar flexion angle increased (caused by increasing wedge height) the cross-correlation values increased mathematically (Figure 5.1)

The Biomechanical Efficiency Quotient (BEQ) is another measure of gait efficiency. The BEQ is the ratio of the measured CoM excursion to the predicted CoM excursion. A larger BEQ indicates a less efficient gait. Notice that as heel wedge height increased, so did the BEQ value (Figure 5.2).

Both the motion capture data and the sensor data measured a decrease in overall gait efficiency with increasing heel wedge height. The values between measurement tools differ for some conditions, but, both tools measured a decrease in efficiency with increasing heel wedge height.

5.2.1 Repeated Measures MANOVA of Efficiency Measures

A 2 X 5 (Measurement Tool X Condition) Repeated Measures Multivariate Analysis of Variance was used to investigate differences in the mean cross-correlation and mean BEQ values. The two measurement tools were the motion capture system and the IMU sensors. The conditions were the five experimental conditions from control to high wedge.

There was a main effect of measurement tool, $F(2,12) = 26.12$ ($p < 0.0001$, $\eta_p^2 = 0.808$) , and condition, $F(6,8) = 89.75$, ($p < 0.0001$, $\eta_p^2 = 0.920$), but no interaction between tool and condition, $F(4,10) = 2.02$, ($p = 0.153$, $\eta_p^2 = 0.447$, post-hoc power = 1.00). Greenhouse-Geiser adjusted post-hoc univariate tests found an effect of condition on both the correlation, $F(2.01,26.14) = 90.92$, ($p < 0.001$), and BEQ, $F(3.98,10.54) = 34.43$ ($p < 0.001$). Pairwise comparisons investigating differences between conditions were performed on estimated marginal means to control for the effect of measurement tool. Pairwise comparisons of cross-correlation values found that the control condition and the zero AFO condition were not different from one another but were less than all other conditions ($p < 0.005$). All other conditions were different from one another ($p < 0.005$) (Figure 5.1). Pairwise comparisons of Biomechanical Efficiency Quotient values found that the control condition, the zero AFO condition and the low wedge conditions were not different from one another, but they were all less than the medium and high wedge conditions ($p < 0.005$; Figure 5.2)

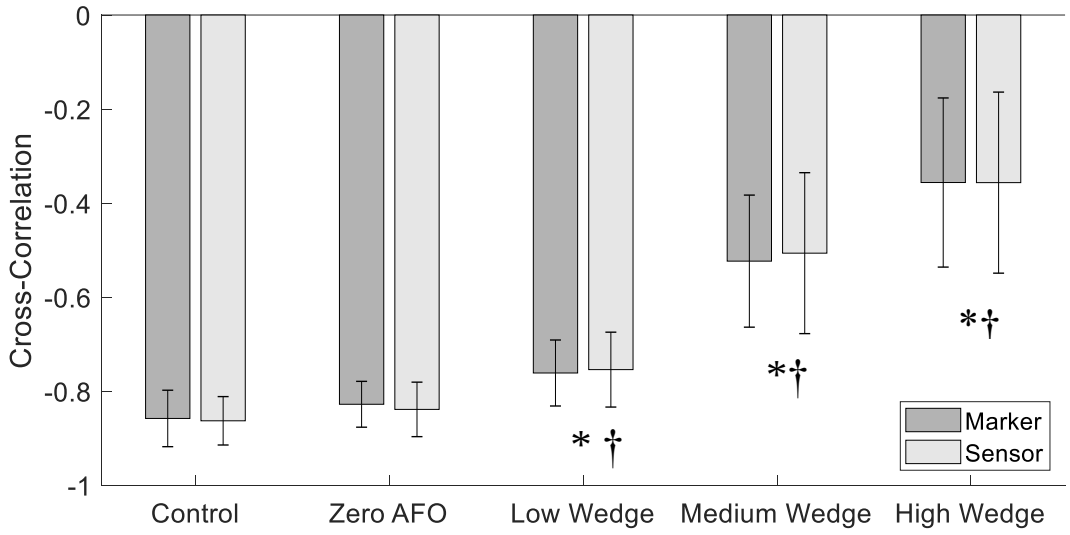

Figure 5.1: Ensemble average (N =14) of the average cross-correlation values with increasing plantar flexion angle. * represents a significant difference from the control condition ($p < 0.05$) and † represents a significant difference the condition to the immediate left ($p < 0.05$).

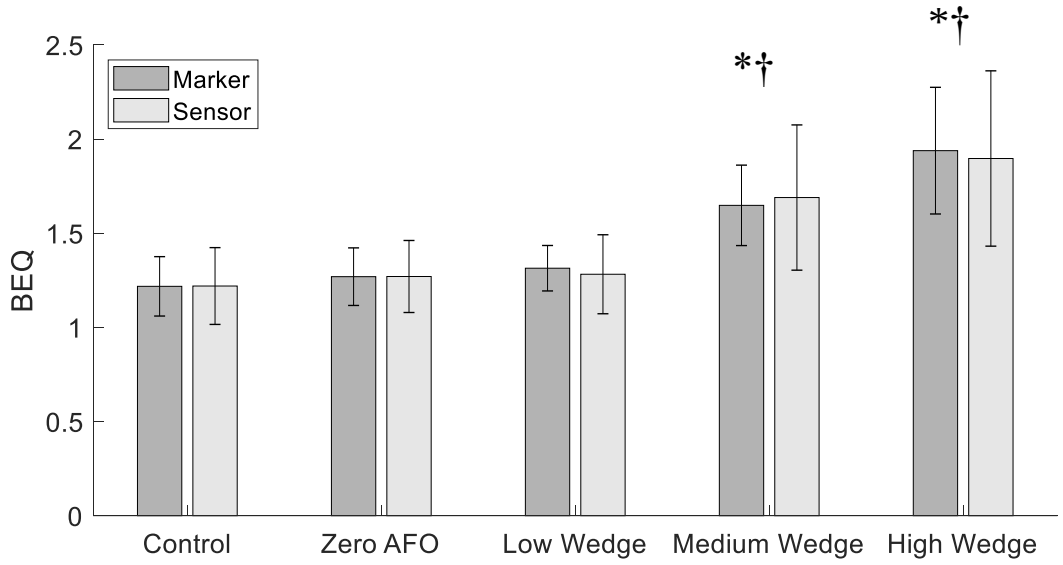

Figure 5.2: Ensemble average (N = 14) of Biomechanical Efficiency Quotient values with increasing heel wedge height. * represents a significant difference from the control condition ($p < 0.05$) and † represents a significant difference the condition to the immediate left ($p < 0.05$).

5.3 Stability Measures

The harmonic ratio (HR) is a measure of gait stability. It is calculated by summing the amplitudes of the odd numbered harmonics and summing the amplitudes of the even numbered harmonics from the acceleration data and calculating the ratio between them. A higher harmonic ratio is indicative of a more stable gait pattern. Note that the control condition had an HR that was higher than the high wedge condition in all directions of motion at both the low back and the head (Figure 5.3 & Figure 5.4). Also, although the values calculated from the sensor and marker data differ, they follow the same trend with changing heel wedge height.

The percent attenuation of the acceleration amplitude from the low back to the head is a measure of stability. An inability to attenuate acceleration from the low back to the head is indicative of decreased stability. Note that there was no change in the percent attenuation of the acceleration amplitude from the low back to the head across all conditions in all three directions of motion for both measurement tools (Figure 5.5).

5.3.1 Repeated Measures MANOVA of Harmonic Ratios at the Low Back

A 2 X 5 (Measurement Tool X Condition) Repeated Measures Multivariate Analysis of Variance was used to investigate differences in the harmonic ratio values of the low back. The two measurement tools were the motion capture system and the IMU sensors. The conditions were the five experimental conditions from control to high wedge.

Main effects of tool, $F(3, 11) = 38.14$ ($p < 0.0001$, $\eta_p^2 = 0.912$), and condition, $F(2,12) = 26.62$. ($p = 0.037$, $\eta_p^2 = 0.994$) were found. There was not an interaction between measurement tool and condition.

$F(2,12) = 5.10$ ($p = 0.18$, $\eta_p^2 = 0.97$ post-hoc power = 1.0). Greenhouse-Geisser corrected post-hoc univariate test found an effect of condition on the harmonic ratios in all directions of motion ($p < 0.0001$). Pairwise comparisons investigating differences between conditions were performed on estimated marginal means to control for the effect of measurement tool.

Pairwise comparisons of the harmonic ratios in the vertical direction at the low back found that the harmonic ratio for the control condition was not different from the zero AFO, but was larger than the low, medium and high wedge conditions ($p < 0.001$). The low wedge condition was larger than the medium and high wedge conditions ($p < 0.0001$). The harmonic ratio value in the vertical direction for the medium wedge condition was also a larger than that of the high wedge condition ($p = 0.01$).

Pairwise comparisons of the harmonic ratios in the anterior-posterior direction at the low back found that the harmonic ratio for the control condition and zero AFO condition were not different from one another but were larger the medium and high wedge conditions ($p < 0.01$). The low wedge condition was larger than both the medium and high wedge conditions ($p < 0.01$).

Pairwise comparisons of the harmonic ratios in the mediolateral direction at the low back found that the harmonic ratio for the control condition was not larger than the zero AFO condition but both the HR values for the control and zero AFO conditions were larger than the medium and high wedge conditions ($p < 0.01$). The low wedge condition was larger than the medium and high wedge conditions ($p < 0.05$).

5.3.2 Repeated Measures MANOVA of Harmonic Ratios at the Head

A 2 X 5 (Measurement Tool X Condition) Repeated Measures Multivariate Analysis of Variance was used to investigate differences in the harmonic ratio values at the head. The two measurement tools were the motion capture system and the IMU sensors. The conditions were the five experimental conditions from control to high wedge.

A main effect of tool, $F(3, 11) = 29.96$ ($p < 0.0001$, $\eta_p^2 = 0.891$), and condition, $F(2, 12) = 83.10$, ($p = 0.01$, $\eta_p^2 = 0.998$) were found. There was not an interaction between tool and condition, $F(2,12) = 2.96$ ($p = 0.28$, $\eta_p^2 = 0.947$, post-hoc power = 0.99). Greenhouse-Geisser corrected post-hoc univariate test found an effect of condition on the harmonic ratios in all directions ($p < 0.0001$).

Pairwise comparisons investigating differences between conditions were performed on estimated marginal means to control for the effect of measurement tool.

Pairwise comparisons of the harmonic ratios in the vertical direction at the head found that the harmonic ratio for the control condition was larger than the low, medium and high wedge conditions ($p < 0.0001$). The harmonic ratio in the vertical direction for the low wedge condition was larger than the medium and high wedge conditions ($p < 0.0001$). The harmonic ratio value in the vertical direction for the medium wedge condition was larger than that of the high wedge condition ($p = 0.02$).

Pairwise comparisons of the harmonic ratios in the forward direction at the head found that the harmonic ratio for the control condition was larger than the medium and high wedge conditions ($p < 0.05$). The low wedge condition was larger the medium and high wedge conditions ($p < 0.05$).

Pairwise comparisons of the harmonic ratios in the mediolateral direction at the head found that the harmonic ratio for the control condition was larger than the medium and high wedge conditions ($p < 0.05$). Also, the harmonic ratio for the zero AFO condition was larger than the high wedge condition ($p = 0.001$).

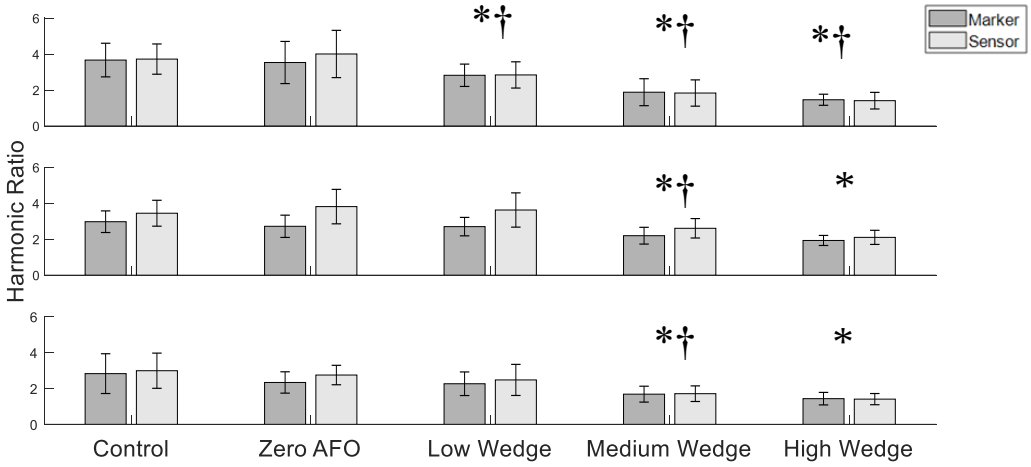

Figure 5.3: Ensemble average (N = 14) of harmonic ratio values of the low back accelerations in the vertical (top), anterior-posterior (middle) and mediolateral (bottom) directions. * represents a significant difference from the control condition ($p < 0.05$) and † represents a significant difference compared to the condition to the immediate left ($p < 0.05$).

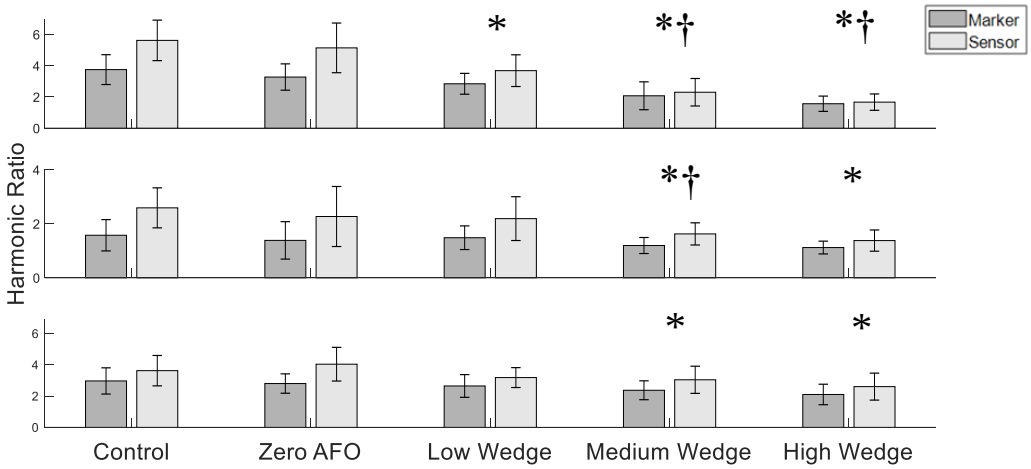

Figure 5.4: Ensemble average (N = 14) of harmonic ratio values of the head accelerations in the vertical (top), anterior-posterior (middle) and mediolateral (bottom) directions. * represents a significant difference from the control condition ($p < 0.05$) and † represents a significant difference compared to the condition to the immediate left ($p < 0.05$).

5.3.3 Repeated Measures MANOVA of Percent Attenuation of Acceleration from Low Back to Head

A 2 X 5 (Measurement tool X Condition) Repeated Measures Multivariate Analysis of Variance was used to investigate differences in percent of acceleration attenuation from the low back to the head in all three directions of motion. The two measurement tools were the motion capture system and the IMU sensors. The conditions were the five experimental conditions from control to high wedge. A main effect of tool, $F(3, 11) = 7.40$ ($p < 0.0001$), was found. There was no effect of condition (Figure 5.5) or an interaction between tool and condition ($p = 0.43$, post-hoc power = 0.99).

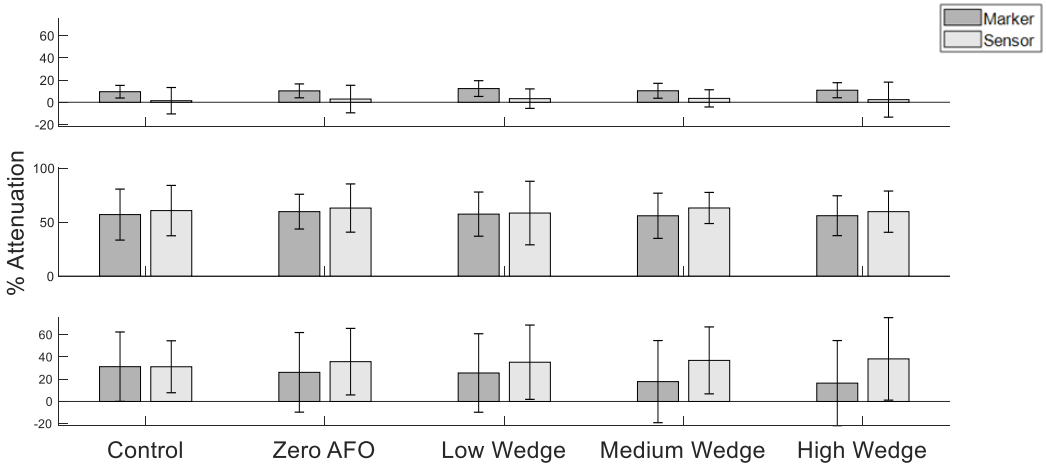

Figure 5.5: Ensemble average (N = 14) of percent attenuation values of accelerations from the low back to the head in the vertical (top), anterior-posterior (middle) and mediolateral (bottom) directions.

5.4 Descriptive Statistics of Efficiency and Stability Survey Results

The survey was intended to provide some insight into the participants' perception of efficiency and stability with increasing heel wedge height. The survey scores for stability showed a trend toward less perceived stability with increasing plantar flexion angle although the variance in scores was large in every condition (Table 5.2). Likewise, the survey scores for efficiency showed a trend

less perceived efficiency with increasing plantar flexion angle but the variance was also large in these responses (Table 5.2).

Table 5.2: Ensemble average and standard deviation (N = 15) of survey scores.

	Zero AFO mean (S.D.)	Low wedge mean (S.D.)	Medium wedge mean (S.D.)	High wedge mean (S.D.)
Stability	6.5 (12.9)	12.9 (19.1)	16.9 (19.8)	21.6 (23.2)
Efficiency	19.2 (17.4)	23.7 (19.4)	25.6 (19.2)	39.2 (21.8)

Note: All question scores were normalized to 100, then related question scores (stability or efficiency) were combined to yield a mean and standard deviation for each condition. Increasing scores indicated more perceived effort and less perceived stability.

5.5 Walking Speed Analysis

Walking speed may influence the efficiency and stability outcome variables of interest. Therefore, the walking speed for each condition was calculated from the motion capture data of the low back marker. Table 5.3 displays the walking speed data.

A one-way repeated measures analysis of variance found an effect of condition on walking speed, $F(4,56) = 7.98$ ($p < 0.0001$, $\eta_p^2 = 0.363$). Bonferroni adjusted post-hoc comparisons found that the walking speeds during the control and zero AFO conditions were faster than the walking speed during the high wedge condition ($p < 0.05$). There were no other differences.

Table 5.3: Ensemble averages of walking speed for each condition.

	Control mean (S.D.)	Zero AFO mean (S.D.)	Low wedge mean (S.D.)	Medium wedge mean (S.D.)	High wedge mean (S.D.)
Speed (m/s)	1.3 (0.2)	1.3 (0.1)	1.3 (0.1)	1.3 (0.3)	1.2 (0.2)

Chapter 6

Discussion

The purpose of this work was to: (1) create a measurable change in gait efficiency and stability that could be detected using motion capture technology; and (2) confirm that similar changes in stability and efficiency are detectable using two IMU sensors, one attached to the lower back at the approximate location of the CoM and one attached to the top of the head.

6.1 General Findings

Both hypotheses were confirmed as increasing plantar flexion angle did cause measurable changes in gait efficiency and stability. Furthermore, there was no significant interaction between measurement tool and condition for any of the outcome measures, suggesting that the changes in efficiency and stability from condition to condition were similar regardless of which measurement tool was used. The nonsignificant interaction between measurement tool and condition supports the second hypothesis that the sensors can measure similar changes in gait efficiency and stability as the motion capture system.

Measurable changes in efficiency and stability were found in all outcome variables except for percent attenuation. The cross-correlation and BEQ values measured a decrease in efficiency, as they both increased with increasing plantar flexion angle. The harmonic ratio values at both the head and the low back decreased in all directions of motion with increasing plantar flexion angle indicating a less stable gait pattern. The percent attenuation of the amplitude of the acceleration from the low back to the head in all three directions of motion did not change with increasing plantar flexion. The results support the use of a two IMU sensor system to measure changes in gait efficiency and stability.

6.2 Efficiency Measures

Recall, in normal efficient gait, we expect a cross-correlation between vertical displacement and forward velocity of the low back to be close to negative one (Figure 2.2; inverse relationship). As the cross-correlation values become less negative, the gait pattern becomes less efficient. In the current work, the cross-correlation between the low back vertical displacement and forward velocity became less negative with increasing plantar flexion angle. There were significant differences between every condition except for between the control condition and the zero AFO condition. During the zero AFO condition the participant was fitted with the AFO, but there were no heel wedges placed underneath the AFO to increase plantar flexion angle, and the strap to limit dorsiflexion was left loose. With no change in efficiency measures between the control and zero AFO conditions, we can conclude that the AFO itself and its fit to the participant did not affect their walking efficiency. Therefore, the measured change in the cross-correlation values between conditions was due to the increasing plantar flexion and restricted dorsiflexion and not due to a poor fit of the AFO or shoe required for the protocol. Bennett et al. (2005) studied the kinetic and potential energy profiles in a population of children with cerebral palsy compared to a population of age-match controls. Bennett found that the kinetic energy curve lagged, in time, behind the potential energy curve leading to less efficient energy recovery and that more mechanical work was required to lift the CoM vertically during the stride cycle (Bennett et al., 2005). Bennett suggested that children with cerebral palsy attempt to employ the same energy saving tradeoff strategy as their able-bodied counterparts but simply execute it more poorly (Bennett et al., 2005). Finally, it was reported that children with cerebral palsy average 60% more CoM excursion vertically than able-bodied children, the energy to raise the CoM is a result of greater work being done by individuals with cerebral palsy One possible explanation for the greater vertical CoM excursion displayed by individuals with cerebral palsy is a lack of knee flexion during the swing phase, which may hamper foot clearance. Therefore, individuals with cerebral palsy tilt their trunk to achieve

foot clearance in the swing phase and tilting the trunk raises the total body CoM (Bennett et al., 2005). The BEQ builds on these concepts by using vertical CoM excursion to draw conclusion on overall gait efficiency.

The BEQ increased with increasing plantar flexion angle. The results from the current work agree with a study that gauged the ability of the of the BEQ to effectively evaluate gait efficiency by testing a control population, a group of individuals with spastic-hemiplegic cerebral palsy and a third group of individuals with spastic diplegic cerebral palsy (Benda et al., 2002). Individuals with spastic diplegia had the least efficient gait, compared to able-bodied individuals (Benda et al., 2002). The results showed that the BEQ was sensitive to efficiency changes and could differentiate between the three groups, from the most efficient, control group, to the least efficient, spastic diplegic group. The BEQ value is dependent on the amount of vertical CoM excursion, as it is the ratio of a predicted value of CoM excursion vertically and the measured excursion. The formula to predict vertical CoM excursion was derived from normative data. Therefore, any gait pattern that has a similar amount of CoM vertical excursion to normal gait will have a BEQ value of one or close to one. Both the BEQ values calculated in the control condition in the current work and the literature found BEQ values for an able-bodied population to be close to one. (Figure 5.2; Benda et al., 2002). In clinical populations the vertical CoM excursion is often greater than that observed in an able-bodied population (Bennett et al., 2005), in these clinical populations, the measured CoM excursion vertically will be greater than the predicted leading to a larger BEQ value. If there is a population that displays a gait pattern with a CoM excursion less than the predicted value, then the BEQ value will be less than one. Minimal movement of the CoM is also known to be the cause of an inefficient gait pattern (Ortega & Farley, 2005). The inverted pendulum-like up and down motion of the CoM is necessary for normal efficient gait, but too much or too little movement can both contribute to a less efficient gait pattern (Gordon et al., 2009; Ortega & Farley, 2005). In a population with greater CoM excursion vertically compared to normal there is an increase in

mechanical work done on the CoM leading to a more costly and less efficient gait (Benda et al., 2002; Bennett et al., 2005).

Although, mechanical cost and metabolic cost are not the same, they are highly corelated (Duff-Raffaele et al., 1996a; Grabowski, Farley, & Kram, 2005). In normal, healthy walkers, 50% of the metabolic cost of gait is dedicated to the mechanical work required to raise the CoM during the stride cycle (Duff-Raffaele, Kerrigan, Corcoran, & Saini, 1996b). Furthermore, BEQ, a measure that compares the actual vertical CoM excursion to a predicted vertical excursion is strongly related to relative VO_2 (Benda et al., 2002). The correlation between the mechanical and metabolic cost of walking provides support that vertical CoM excursion is a good predictor of overall cost of gait and is the foundation of the two efficiency outcome measures used in the current work.

6.3 Stability Measures

In all directions of motion at the low back and the head, the harmonic ratio values decreased from the control condition to the high wedge condition. Although, the harmonic ratio values were less sensitive to changes than the efficiency measures, as sometimes differences were not found between the control, low and medium wedge conditions. This could be because (1) the measure of harmonic ratio is less sensitive to changes in stability or (2) the increase in plantar flexion angle had less of an effect on stability than it did on efficiency. The latter seems more likely as the participant population was able-bodied and was, therefore, likely able to adapt to the forced changes to their gait pattern. Further, the AFO and heel wedge setup, although it allowed for the control and modification of plantar flexion angle during gait, provided support under the midfoot and heel that in turn may have made the participant more stable compared to an individual walking on their toes. But, in all cases the harmonic ratio in the control condition was significantly greater than the harmonic ratio calculated for the medium and high wedge conditions in all directions of motion.

A notable limitation of the harmonic ratio is that it is confounded by walking speed. It has been reported that lower harmonic ratio values will be found at slower walking speeds independent of

any gait limitation or perturbation (Bellanca, Lowry, VanSwearingen, Brach, & Redfern, n.d.). Walking speed was not controlled in the current work; participants walked a self-selected pace. Analysis of walking speed across conditions (Table 5.3) found that the average walking speed in the high wedge condition was significantly slower than in the control and zero AFO conditions, but there were no other significant differences of walking speed among the conditions. The differences found, although significant, were very small, therefore, it seems reasonable to conclude that the differences found were, at least in part, due to the increase in plantar flexion angle.

There was no effect of increasing plantar flexion angle on the amount of attenuation of acceleration from the low back to the head. This may be because the population used in the study were able-bodied individuals who had no deficit to their core muscles. Previous research has found that attenuation of acceleration from the lower body to the head is controlled by the coordinated contraction of paraspinal muscles from the lower back to the head (Prince et al., 1994). Other studies have shown a decrease in the ability to attenuate accelerations from the lower body to the head in populations who have trunk weakness (Buckley et al., 2015). Considering the support of previous research on clinical populations, and that the motion capture data and sensor data both showed the result of no effect, we still believe that the acceleration attenuation from the low back to the head is clinically useful from a stability perspective.

6.4 Survey Results

The efficiency and stability survey provided some insight into the participant's perception of effort and their stability during the different conditions. The mean efficiency and stability survey scores followed the same trends as the outcome variables for both stability and efficiency of decreasing stability and efficiency, but the standard deviations were large. Therefore, it is difficult to draw any meaningful conclusions from the survey data. A limitation to the efficacy of the survey was that the only scale used that had been validated by research was the Borg scale. But, the Borg scale has been shown to be less reliable during low intensity exercise, such as the walking protocol

in the current work (Eston & Williams, 1988; Ritchie, 2012). The reduced reliability of the Borg scale at lower intensity exercises coupled with lack of other valid and reliable scales to subjectively measure efficiency and stability may have affected the survey results. To our knowledge there is currently no tested and reliable scale to measure perceived dynamic stability. Future work should aim to measure perceived stability and efficiency with valid, reliable subjective measurement tools and compare to objective measures to confirm that participants are feeling the effects of the changes in stability and efficiency that are being measured.

6.5 Sensor Processing

As outlined in chapter 3, finding the best processing technique for the sensor data to yield results best matching the motion capture data was one of the biggest challenges in the current work. Most of the processing techniques found in the literature involved selecting high pass and low pass filter cut-offs for the sensor acceleration data that allowed the sensor data to be processed to yield the best match to the marker data. In other words, motion capture data was needed to successfully obtain accurate velocities and displacement values from the sensor data. Such techniques will not be useful in the field, where a comparison to motion capture data is not possible. For the above techniques to be useful in the field, a method of selecting optimal filter cut-offs on a case-by-case basis solely from the sensor data is required. To our knowledge no such technique currently exists.

For the reasons stated in the preceding paragraph the Fourier-based signal reconstruction and integration technique (Sabatini et al., 2015) was selected to process the sensor data in the current work. The Fourier-based signal reconstruction and integration technique mitigates signal drift by using Fourier coefficients from the acceleration data to reconstruct the acceleration, velocity and displacement curves. Although it was selected as the most suitable processing technique for the current work, the Fourier based integration of the acceleration signals was not without limitations. One major limitation was the requirement for the signal to be periodic (Sabatini et al., 2015). For the signal to be considered periodic, it must repeat at regular intervals. The requirement for the

signal to be periodic is met in almost all cases by completing the analysis stride-by-stride. But forward displacement cannot be periodic as its initial and final conditions are not equal. This causes issues in studies such as ours which rely on the accurate calculation of stride length as an intermediate calculation of an outcome variable (BEQ).

A few different attempts of calculating stride length from the low back sensor were explored but proved to be unreliable from participant to participant. Therefore, the method of dividing the known distance walked by the number of steps taken and multiplying by two was used (Menz et al., 2003b). Although, this method yields accurate results it imposes a minor constraint on the use of the current methods in the field. The requirement to measure a distance is an inconvenience and should not be necessary. A method of accurately measuring stride length from a single sensor attached to the approximate location of CoM would be ideal, but to our knowledge no such method exists. Adapting our current system to include a third sensor on the shank, or the foot solely for the purpose of measuring stride length would be a suitable solution (Kasai et al., 2017; Sijobert et al., 2015).

6.6 Limitations

The limitations in the current work are due to laboratory setup, the IMU sensors, and AFO design. One of the major limitations was the small calibrated motion tracking space within the lab that was able to collect motion capture data. The length of this space allowed, at most, one left and one right stride for each participant per trial. A setup where the motion capture data could be collected for the same number of steps as the sensor data would allow a better comparison between motion capture and sensor data, rather than only being able to compare mean strides between tools.

The next limitations are due to the design of the AFO to manipulate plantar flexion angle. The AFO did not mimic the gait of someone with foot equinus as the wedge provided support under the midfoot and heel, which limited our ability to compare our results to those of individuals with foot equinus. Although, coaching participants to walk on their toes on one side was an option for the

current work (D. C. Kerrigan, Riley, Rogan, & Burke, 2000), such methods would cause the loss of regulation and control of the plantar flexion angle. Furthermore, there were only two sizes of AFOs and two sizes of shoes, and although the best fit was always selected for the participant, the setup fit everyone differently, causing slight changes in the plantar flexion angle between individuals that may have affected the results as the conditions may not have been consistent between participants. These limitations need to be noted, as they may have affected the results, but the AFO design was suitable for this project and its purposes.

Sensor technology also limited the current work. Bluetooth download error sometimes required recollecting a condition for a participant. This extra repetition may have induced some learning by the participants and confounded the results over and above the innate limitation of learning found in repeated-measures designs (Singh, Rana, & Singhal, 2013). Moreover, inherent software issues with the sensors may limit their usefulness as a clinical tool. It is imperative that the sensors and their software be dependable and user friendly.

6.7 Future Directions

Future studies should test the proposed two IMU sensor system on different clinical populations to verify its ability to detect changes in efficiency and stability. With the change in gait patterns displayed in clinical populations compared to able-bodied individuals, it is possible that some of the algorithms and processing techniques (i.e. separating data into strides) may need to be altered to be useful for other populations. Furthermore, although most of the outcome variables have been used in previous studies and have shown promising results with clinical population, these previous studies did not calculate the outcome variables using IMU sensors (except for harmonic ratio and percent attenuation). Calculating the outcome variables in the current work using the two-sensor system on different clinical populations is vital to ensure the system can measure changes in the outcome variables for different populations.

Finally, the development of a smartphone application would make the tool more accessible and useful to clinical professionals. Once developed, the application would make the proposed system more user friendly, allowing clinical professionals to obtain objective measures of stability and efficiency, giving them the ability to monitor changes in their client's gait efficiency and stability.

6.8 Conclusions

Increasing the plantar flexion angle on the right side, caused measurable changes in gait efficiency and stability in a population of able-bodied individuals. The BEQ and cross-correlation values measured a decrease in efficiency. The harmonic ratio values at both the head and the low back decreased in all directions of motion with increasing plantar flexion angle indicating a less stable gait pattern. The percent attenuation of the amplitude of the acceleration from the low back to the head in all three directions of motion did not change with increasing plantar flexion. Finally, the two IMU sensor system measured similar changes in gait efficiency and stability when compared to the motion tracking system.

This work took the first steps to create a simple two-sensor system to measure efficiency and stability of gait. Efficiency and stability are two objective and clinically relevant variables that when combined with the subjective analysis presently used in clinic will help formulate a more holistic view of an individual's gait.

Bibliography

Abdi, H., & Williams, L. J. (2010). Principal component analysis. *Wiley Interdisciplinary Reviews: Computational Statistics*, *2*(4), 433–459. https://doi.org/10.1002/wics.101

American College of Rheumatology. (2015). Six Minute Walk Test (6MWT). Retrieved October 16, 2018, from https://www.rheumatology.org/I-Am-A/Rheumatologist/Research/Clinician-Researchers/Six-Minute-Walk-Test-SMWT

Bache, C. E., Selber, P., & Graham, H. K. (2003). The management of spastic diplegia. *Current Orthopaedics*, *17*(2), 88–104. https://doi.org/10.1054/cuor.2003.0328

Bellanca, J., Lowry, K., VanSwearingen, J., Brach, J., & Redfern, M. (n.d.). Harmonic ratios: A quantification of step to step symmetry. https://doi.org/10.1016/j.jbiomech.2012.12.008

Benda, B. J., Smith, B. T., & Lange, G. W. (2002). Evaluating the effectiveness of the biomechanical efficiency quotient as a me children with cerebral palsy, 2–3.

Bennett, B. C., Abel, M. F., Wolovick, A., Franklin, T., Allaire, P. E., & Kerrigan, D. C. (2005). Center of mass movement and energy transfer during walking in children with cerebral palsy. *Archives of Physical Medicine and Rehabilitation*, *86*(11), 2189–2194. https://doi.org/10.1016/j.apmr.2005.05.012

Bolster, E. A. M., Balemans, A. C. J., Brehm, M. A., Buizer, A., & Dallmeijer, A. J. (2017). Energy cost during walking in association with age and body height in children and young adults with cerebral palsy. *Gait and Posture*, *54*, 119–126. https://doi.org/10.1016/j.gaitpost.2017.02.026

Bonnyaud, C., Pradon, D., Bensmail, D., & Roche, N. (2015). Dynamic stability and risk of tripping during the timed up and go test in hemiparetic and healthy subjects. *PLoS ONE*, *10*(10), 1–14. https://doi.org/10.1371/journal.pone.0140317

Buckley, C., Galna, B., Rochester, L., & Mazzà, C. (2015). Attenuation of Upper Body Accelerations during Gait: Piloting an Innovative Assessment Tool for Parkinson's Disease. *BioMed Research International*, *2015*. https://doi.org/10.1155/2015/865873

Burdett, R. G., Skrinar, G. S., & Simon, S. R. (1983). Comparison of mechanical work and metabolic energy consumption during normal gait. *Journal of Orthopaedic Research*, *1*(1), 63–72. https://doi.org/10.1002/jor.1100010109

Carey, H., Martin, K., Combs-Miller, S., & Heathcock, J. C. (2016). Reliability and responsiveness of the timed up and go test in children with cerebral palsy. *Pediatric Physical Therapy*, *28*(4), 401–408. https://doi.org/10.1097/PEP.0000000000000301

Cavagna, G. A., Heglund, N. C., & Taylor, C. R. (1977). Mechanical work basic mechanisms in terrestrial locomotion : two for minimizing energy expenditure. *The American Journal of Physiology*, *233*(5), 243–261.

Cavagna, G. A., & Kaneko, M. (1977). Mechanical work and efficiency in level walking and running. *The Journal of Physiology*, *268*(2), 467–481. https://doi.org/10.1113/jphysiol.1977.sp011866

Donelan, J. M., Shipman, D. W., Kram, R., & Kuo, A. D. (2004). Mechanical and metabolic requirements for active lateral stabilization in human walking. *Journal of Biomechanics*, *37*(6), 827–835. https://doi.org/10.1016/j.jbiomech.2003.06.002

Duff-Raffaele, M., Kerrigan, C. D., Corcoran, P. J., & Saini, M. (1996a). The Proportional Work of Lifting the Center of Mass During Walking. *American Journal of Physical Medicine*, *75*(5), 375–379.

Duff-Raffaele, M., Kerrigan, D. C., Corcoran, P. J., & Saini, M. (1996b). The proportional work of lifting the center of mass during walking. *American Journal of Physical Medicine and Rehabilitation*, *75*(5), 375–379. https://doi.org/10.1097/00002060-199609000-00014

Duffy, C. M., Hill, a E., Cosgrove, a P., Corry, I. S., & Graham, H. K. (1996). Energy consumption in children with spina bifida and cerebral palsy: a comparative study. *Developmental Medicine and Child Neurology*, *38*(3), 238–243.

Eston, R. G., & Williams, J. G. (1988). Reliability of ratings of perceived effort regulation of exercise intensity. *British Journal of Sports Medicine*, *22*(4), 153–155. https://doi.org/10.1136/bjsm.22.4.153

Gage, J. R. (1993). Gait analysis. An essential tool in the treatment of cerebral palsy. *Clinical Orthopaedics and Related Research*.

Gordon, K. E., Ferris, D. P., & Kuo, A. D. (2009). Metabolic and Mechanical Energy Costs of Reducing Vertical Center of Mass Movement During Gait. *Archives of Physical Medicine and Rehabilitation*, *90*(1), 136–144. https://doi.org/10.1016/j.apmr.2008.07.014

Grabowski, A., Farley, C. T., & Kram, R. (2005). Independent metabolic costs of supporting body weight and accelerating body mass during walking. *Journal of Applied Physiology*, *98*(2), 579–583. https://doi.org/10.1152/japplphysiol.00734.2004

Houx, L., Lempereur, M., Rémy-Néris, O., & Brochard, S. (2013). Threshold of equinus which alters biomechanical gait parameters in children. *Gait and Posture*, *38*(4), 582–589. https://doi.org/10.1016/j.gaitpost.2013.01.026

Huang, T. -w. P., Shorter, K. A., Adamczyk, P. G., & Kuo, A. D. (2015). Mechanical and energetic consequences of reduced ankle plantar-flexion in human walking. *Journal of Experimental Biology*, *218*(22), 3541–3550. https://doi.org/10.1242/jeb.113910

Jolliffe, I. T. (2002). *Principle Component Analysis*. *Springer*. https://doi.org/10.2307/1270093

Jones, J., & McLaughlin, J. F. (1993). Mechanical efficiency of children with spastic cerebral palsy. *Developmental Medicine and Child Neurology*, *35*(7), 614–620. Retrieved from http://www.embase.com/search/results?subaction=viewrecord&from=export&id=L2320634 9%5Cnhttp://openurl.ac.uk/ukfed:bath.ac.uk?sid=EMBASE&issn=00121622&id=doi:&atitl e=Mechanical+efficiency+of+children+with+spastic+cerebral+palsy&stitle=DEV.+MED.+ CHILD+NEUROL

Kasai, R., Kodama, T., Gu, Z., Zhang, D., Kong, W., Cosentino, S., … Takanishi, A. (2017). Reliability of stride length estimation in self-pace and brisk walking with an inertial measurement unit on shank. *2017 IEEE International Conference on Mechatronics and Automation, ICMA 2017*, (May), 671–676. https://doi.org/10.1109/ICMA.2017.8015896

Kerrigan, D. C., Riley, P. O., Rogan, S., & Burke, D. T. (2000). Compensatory advantages of toe walking. *Archives of Physical Medicine and Rehabilitation*, *81*(1), 38–44. https://doi.org/10.1016/s0003-9993(00)90219-3

Kerrigan, D., Thirunarayan, Mandyam Sheffler, L., Ribaudo, T., & Corcoran, P. (1996). A tool to assess your Biomechanical Gait Efficiency: A Preliminary Clinical Study. *American Journal of Physical Medicine*, *75*(1), 3–8.

Köse, A., Cereatti, A., & Della Croce, U. (2012). Bilateral step length estimation using a single inertial measurement unit attached to the pelvis. *Journal of NeuroEngineering and Rehabilitation*, *9*(1), 9. https://doi.org/10.1186/1743-0003-9-9

Kuo, A. D. (2007). The six determinants of gait and the inverted pendulum analogy: A dynamic walking perspective. *Human Movement Science*, *26*(4), 617–656.

https://doi.org/10.1016/j.humov.2007.04.003

Kurz, M. J., Stuberg, W. A., & DeJong, S. L. (2010). Mechanical work performed by the legs of children with spastic diplegic cerebral palsy. *Gait and Posture*, *31*(3), 347–350. https://doi.org/10.1016/j.gaitpost.2009.12.004

Latash, M. (2012). *Fundamentals of Motor Control* (1st ed.). Academic Press.

Latt, M. D., Menz, H. B., Fung, V. S., & Lord, S. R. (2008). Walking speed, cadence and step length are selected to optimize the stability of head and pelvis accelerations. *Experimental Brain Research*, *184*(2), 201–209. https://doi.org/10.1007/s00221-007-1094-x

Lazzer, S., Boirie, Y., Bitar, A., Petit, I., Meyer, M., & Vermorel, M. (2005). Relationship between percentage of V̇O2max and type of physical activity in obese and non-obese adolescents. *Journal of Sports Medicine and Physical Fitness*, *45*(1), 13–19.

Mackey, A. H., Lobb, G. L., Walt, S. E., & Stott, N. S. (2003). Reliability and validity of the Observational Gait Scale in children with spastic diplegia. *Developmental Medicine and Child Neurology*, *45*(1), 4–11. https://doi.org/10.1111/j.1469-8749.2003.tb00852.x

MacKinnon, C. D., & Winter, D. A. (1993). Control of whole body balance in the frontal plane during human walking. *Journal of Biomechanics*, *26*(6), 633–644. https://doi.org/10.1016/0021-9290(93)90027-C

Madgwick, S. O. H. (2014). AHRS algorithms and calibration solutions to facilitate new applications using low-cost MEMS, (March), 273.

Manning, W. J. (2005). Length dependence of active force production in skeletal muscle. *Applied Physiology*, *138*(3), 377. https://doi.org/10.1016/j.envpol.2004.10.021

Meichtry, A., Romkes, J., Gobelet, C., Brunner, R., & Müller, R. (2007). Criterion validity of 3D trunk accelerations to assess external work and power in able-bodied gait. *Gait and Posture*, *25*(1), 25–32. https://doi.org/10.1016/j.gaitpost.2005.12.016

Menard, M. R., Penn, A. M., Lee, J. W. K., Dusik, L. A., & Hall, L. D. (1991). Relative metabolic efficiency of concentric and eccentric exercise determined by 31P magnetic resonance spectroscopy. *Archives of Physical Medicine and Rehabilitation*, *72*(12), 976–983. https://doi.org/10.5555/uri:pii:000399939190139A

Menz, H. B., Latt, M. D., Tiedemann, A., Kwan, M. M. S., & Lord, S. R. (2004). Reliability of the GAITRite® walkway system for the quantification of temporo-spatial parameters of gait in young and older people. *Gait and Posture*, *20*(1), 20–25. https://doi.org/10.1016/S0966-6362(03)00068-7

Menz, H. B., Lord, S. R., & Fitzpatrick, R. C. (2003a). Acceleration patterns of the head and pel v is when walking on le v el and irregular surfaces. *Gait & Posture*, *18*(1), 35–46. https://doi.org/10.1093/gerona/58.5.M446

Menz, H. B., Lord, S. R., & Fitzpatrick, R. C. (2003b). Acceleration patterns of the head and pelvis when walking are associated with risk of falling in community-dwelling older people. *J Gerontol A Biol Sci Med Sci*, *58*(5), M446–M452. https://doi.org/10.1093/gerona/58.5.m446

Menz, H. B., Lord, S. R., & Fitzpatrick, R. C. (2003c). Age-related differences in walking stability. *Age and Ageing*, *32*(2), 137–142. https://doi.org/10.1093/ageing/32.2.137

Menz, H. B., Lord, S. R., St George, R., & Fitzpatrick, R. C. (2004). Walking Stability and Sensorimotor Function in Older People with Diabetic Peripheral Neuropathy. *Archives of Physical Medicine and Rehabilitation*, *85*(2), 245–252.

https://doi.org/10.1016/j.apmr.2003.06.015

Mignardot, J. B., Deschamps, T., Barrey, E., Auvinet, B., Berrut, G., Cornu, C., … De Decker, L. (2014). Gait disturbances as specific predictive markers of the first fall onset in elderly people: A two-year prospective observational study. *Frontiers in Aging Neuroscience*, *6*(FEB), 1–13. https://doi.org/10.3389/fnagi.2014.00022

Murray, M. . (1967). Gait as a Total Patern of Movement. *American Journal of Physical Medicine*, *46*(1), 290–333.

Norman, J. F., Bossman, S., Gardner, P., & Moen, C. (2004). Comparison of the energy expenditure index and oxygen consumption index during self-paced walking in children with spastic diplegia cerebral palsy and children without physical disabilities. *Pediatric Physical Therapy*, *16*(4), 206–211. https://doi.org/10.1097/01.PEP.0000145930.84009.23

Ortega, J. D., & Farley, C. T. (2005). Minimizing center of mass vertical movement increases metabolic cost in walking. *Journal of Applied Physiology*, *99*(6), 2099–2107. https://doi.org/10.1152/japplphysiol.00103.2005

Perry, J. (1992). *Gait Analysis: Normal and Pathological Function*. Thorofare, NJ: SLACK Incorporated.

Peyrot, N., Thivel, D., Isacco, L., Morin, J.-B., Duche, P., & Belli, A. (2009). Do mechanical gait parameters explain the higher metabolic cost of walking in obese adolescents? *Journal of Applied Physiology*, *106*(6), 1763–1770. https://doi.org/10.1152/japplphysiol.91240.2008

Pozzo, T., Berthoz, A., Lefort, L., & Vitte, E. (1991). Head stabilization during various locomotor tasks in humans - II. Patients with bilateral peripheral vestibular deficits. *Experimental Brain Research*, *85*(1), 208–217. https://doi.org/10.1007/BF00230002

Prince, F., Winter, D., Stergiou, P., & Walt, S. (1994). Anticipatory control of upper body balance during human locomotion. *Gait and Posture*, *2*(1), 19–25. https://doi.org/10.1016/0966-6362(94)90013-2

Ries, A. J., & Schwartz, M. H. (2017). Low gait efficiency is the primary reason for the increased metabolic demand during gait in children with cerebral palsy. *Human Movement Science*, *57*(October 2017), 426–433. https://doi.org/10.1016/j.humov.2017.10.004

Ritchie, C. (2012). Rating of Perceived Exertion (RPE). *Journal of Physiotherapy*, *58*(1), 62. https://doi.org/10.1016/S1836-9553(12)70078-4

Sabatini, A. M., Ligorio, G., & Mannini, A. (2015). Fourier-based integration of quasi-periodic gait accelerations for drift-free displacement estimation using inertial sensors. *BioMedical Engineering Online*, *14*(1), 1–18. https://doi.org/10.1186/s12938-015-0103-8

Saleh, M., & Murdoch, G. (1985). In defence of gait analysis. Observation and measurement in gait assessment. *Journal of Bone and Joint Surgery - Series B*, *67*(2), 237–241. https://doi.org/10.1302/0301-620x.67b2.3980533

Shumway-Cook, A., Baldwin, M., Polissar, N. L., & Grubar, W. (1997). Predicting the probability of falls in community-dwelling older adults. *Physical Therapy*, *77*(8), 812–819.

Sijobert, B., Benoussaad, M., Denys, J., Pissard-Gibollet, R., Geny, C., & Azevedo Coste, C. (2015). Open Archive Toulouse Archive Ouverte (OATAO) Implementation and Validation of a Stride Length Estimation Algorithm, Using a Single Basic Inertial Sensor on Healthy Subjects and Patients Suffering from Parkinson's Disease. *Health*, *07*, 6. https://doi.org/10.4236/health.2015.76084

Singh, V., Rana, R. K., & Singhal, R. (2013). Analysis of repeated measurement data in the

clinical trials. *Journal of Ayurveda and Integrative Medicine*, *4*(2), 77–81. https://doi.org/10.4103/0975-9476.113872

Smidt, G. L., Arora, J., & Johnston, R. (1971). Accelerographic analysis of serveral types of walking.

Smidt, G. L., Deusinger, R. H., Arora, J., & Albright, J. P. (1971). an Automated Accelerometry Analysis * System for. *Journal of Biomechanics*, *10*(1), 367–375.

Smith, L. (2006). A tutorial on PCA. *Department of Computer Science, University of Otago.*, 12–28. https://doi.org/http://www.cs.otago.ac.nz/research/techreports.php

Storey, B. B. D. (n.d.). Computing Fourier Series and Power Spectrum with MATLAB. *Time*, 1–15.

Tamura, T. (2005). Wearable accelerometer in clinical use. *Annual International Conference of the IEEE Engineering in Medicine and Biology - Proceedings*, *7 VOLS*, 7165–7166. https://doi.org/10.1109/iembs.2005.1616160

Tao, W., Liu, T., Zheng, R., & Feng, H. (2012). Gait analysis using wearable sensors. *Sensors*, *12*(2), 2255–2283. https://doi.org/10.3390/s120202255

Van Den Hecke, A., Malghem, C., Renders, A., Detrembleur, C., Palumbo, S., & Lejeune, T. M. (2007). Mechanical work, energetic cost, and gait efficiency in children with cerebral palsy. *Journal of Pediatric Orthopaedics*, *27*(6), 643–647. https://doi.org/10.1097/BPO.0b013e318093f4c3

Winter, D. A. (1979). A new definition of mechanical work done in human movement. *Journal of Applied Physiology*, *46*(1), 79–83. https://doi.org/10.1152/jappl.1979.46.1.79

Woollacott, M. H., & Tang, P. F. (1997). Balance control during walking in the older adult: Research and its implications. *Physical Therapy*, *77*(6), 646–660. https://doi.org/10.1093/ptj/77.6.646

Wren, T. A. L., Gorton, G. E., Õunpuu, S., & Tucker, C. A. (2011). Efficacy of clinical gait analysis: A systematic review. *Gait and Posture*, *34*(2), 149–153. https://doi.org/10.1016/j.gaitpost.2011.03.027

Wren, T. A. L., Rethlefsen, S. A., Healy, B. S., Do, K. P., Dennis, S. W., & Kay, R. M. (2005). Reliability and validity of visual assessments of gait using a modified physician rating scale for crouch and foot contact. *Journal of Pediatric Orthopaedics*, *25*(5), 646–650. https://doi.org/10.1097/01.mph.0000165139.68615.e4

Zijlstra, W. (2004). Assessment of spatio-temporal parameters during unconstrained walking. *European Journal of Applied Physiology*, *92*(1–2), 39–44. https://doi.org/10.1007/s00421-004-1041-5

Zok, M., Mazzà, C., & Della Croce, U. (2004). Total body centre of mass displacement estimated using ground reactions during transitory motor tasks: Application to step ascent. *Medical Engineering and Physics*, *26*(9 SPEC.ISS.), 791–798. https://doi.org/10.1016/j.medengphy.2004.07.005

Appendices

Appendix A
Example: Acceleration, Velocity and Displacement Data

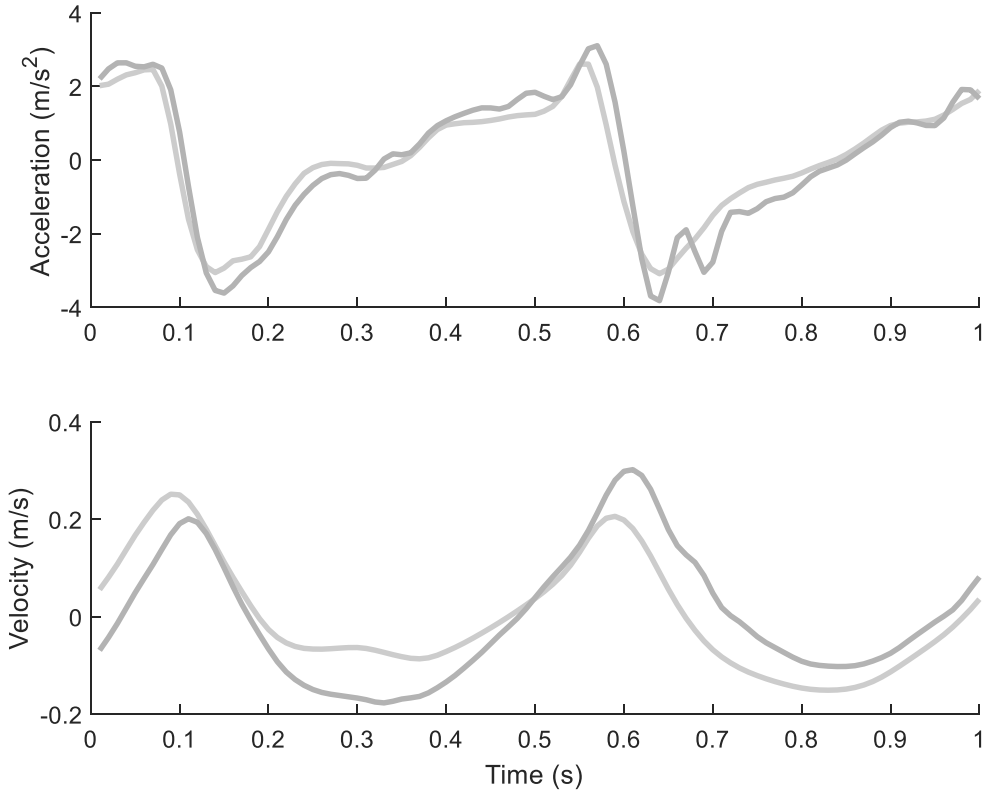

Figure A.1: Average forward acceleration and velocity of the CoM data of all strides for one participant. Marker data (light grey) and sensor data (dark grey) are plotted against time. Time was normalized to one second.

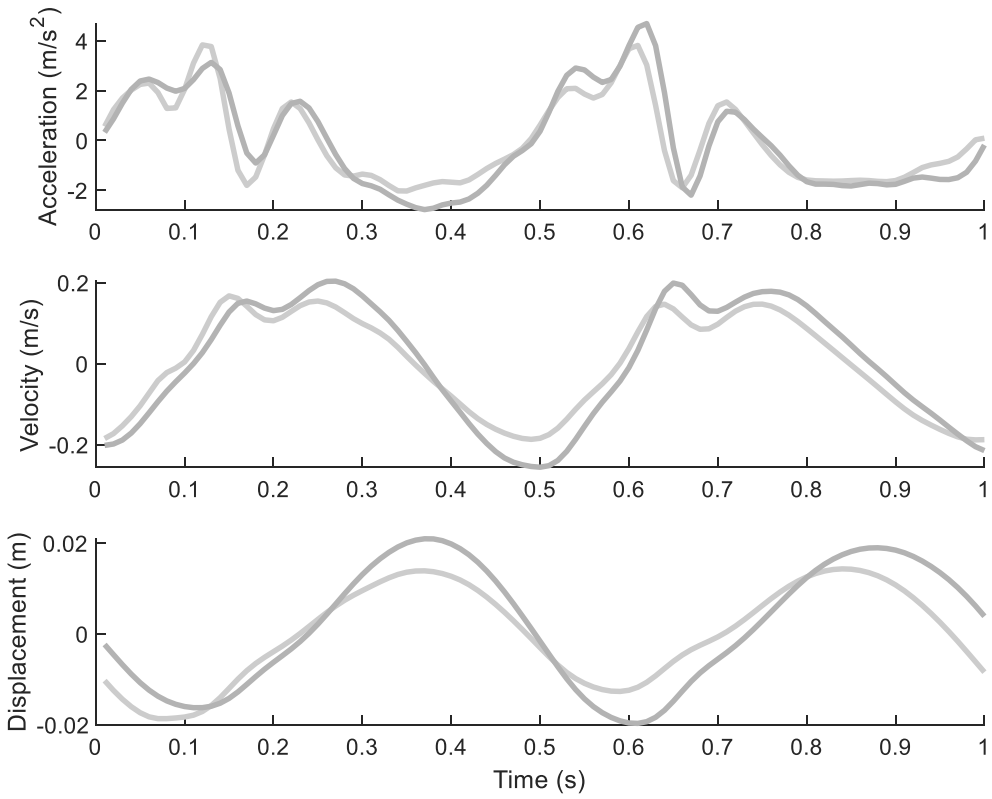

Figure A.2: Average vertical acceleration, velocity and displacement of the low back data of all strides for one participant. Marker data (light grey) and sensor data (dark grey) are plotted against time. Time was normalized to one second.

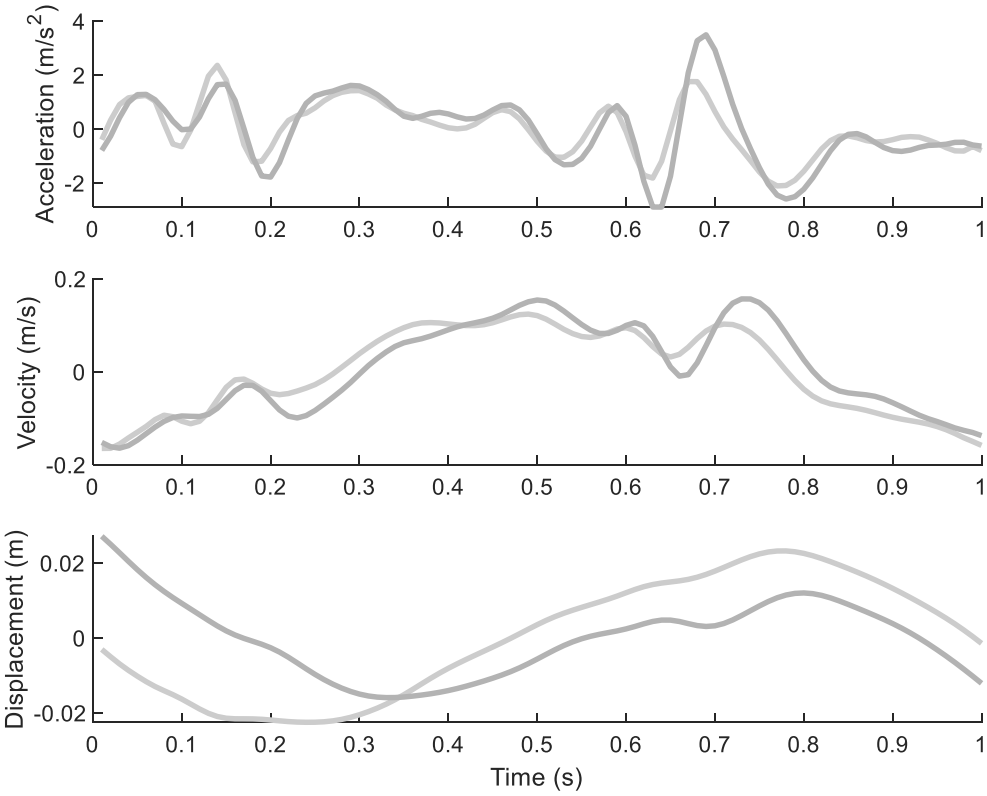

Figure A.3: Average mediolateral acceleration, velocity, and displacement of the low back data of all strides for one participant. Marker data (light grey) and sensor data (dark grey) are plotted against time. Time was normalized to one second.

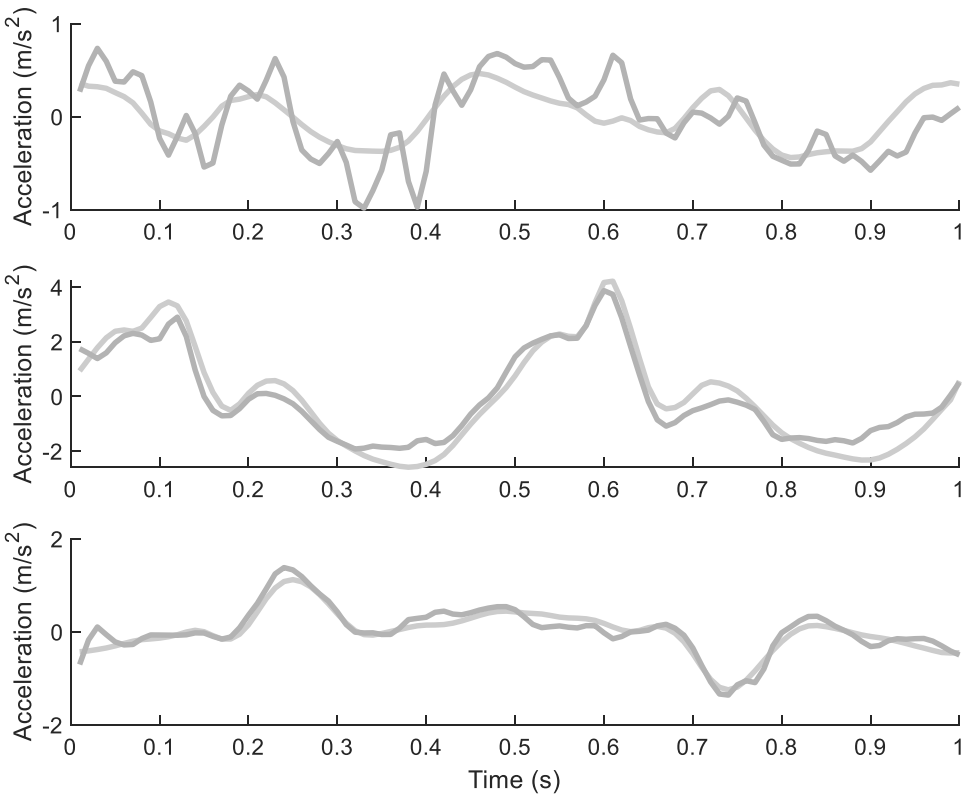

Figure A.4: Average acceleration in the forward (top, vertical (middle) and mediolateral (bottom) directions of the head data of all strides for one participant. Marker data (light grey) and sensor data (dark grey) are plotted against time. Time was normalized to one second.

Appendix B

Ethics Approval and Amendments

January 29, 2019

Mr. Joshua Davies
Master's Student
School of Kinesiology and Health Studies
Queen's University
28 Division Street
Kingston, ON, K7L
3N6

GREB Ref #: GSKHS-305-18; TRAQ # 6025645
Title: "GSKHS-305-18 Investigating Efficiency and Stability of Gait using a Two Triaxial Sensor System"

Dear Mr. Davies:

The General Research Ethics Board (GREB), by means of a delegated board review, has cleared your proposal entitled **"GSKHS-305-18 Investigating Efficiency and Stability of Gait using a Two Triaxial Sensor System"** for ethical compliance with the Tri-Council Guidelines (TCPS 2 (2014)) and Queen's ethics policies. In accordance with the Tri-Council Guidelines (Article 6.14) and Standard Operating Procedures (405.001), your project has been cleared for one year. You are reminded of your obligation to submit an annual renewal form prior to the annual renewal due date (access this form at http://www.queensu.ca/traq/signon.html/; click on "Events;" under "Create New Event" click on "General Research Ethics Board Annual Renewal/Closure Form for Cleared Studies"). Please note that when your research project is completed, you need to submit an Annual Renewal/Closure Form in Romeo/traq indicating that the project is 'completed' so that the file can be closed. This should be submitted at the time of completion; there is no need to wait until the annual renewal due date.

You are reminded of your obligation to advise the GREB of any adverse event(s) that occur during this one-year period (access this form at http://www.queensu.ca/traq/signon.html/; click on "Events;" under "Create New Event" click on "General Research Ethics Board Adverse Event Form"). An adverse event includes, but is not limited to, a complaint, a change or unexpected event that alters the level of risk for the researcher or participants or situation that requires a substantial change in approach to a participant(s). You are also advised that all adverse events must be reported to the GREB within 48 hours.

You are also reminded that all changes that might affect human participants must be cleared by the GREB. For example, you must report changes to the level of risk, applicant characteristics, and implementation of new procedures. To submit an amendment form, access the application by at http://www.queensu.ca/traq/signon.html; click on "Events;" under "Create New Event" click on "General Research Ethics Board Request for the Amendment of Approved Studies." Once submitted, these changes will automatically be sent to the Ethics Coordinator, Ms. Gail Irving, at University Research Services for further review and clearance by the GREB or Chair, GREB.

On behalf of the General Research Ethics Board, I wish you continued success in your research. Sincerely,

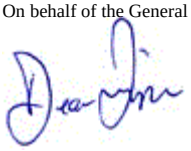

Dean Tripp,
Ph.D. Chair
General Research Ethics Board

c: Dr. Patrick Costigan, Supervisor
Dr. Elaine Power, Chair, Unit REB
Ms. Josie Birchall, Dept. Admin.

April 02, 2019

Mr. Joshua Davies
Master's Student
School of Kinesiology and Health Studies Queen's University
28 Division Street Kingston, ON,
K7L 3N6

Dear Mr. Davies:

RE: Amendment for your study entitled**: GSKHS-305-18 Investigating Efficiency and Stability of Gait using a Two Triaxial Sensor System;** TRAQ **# 6025645**

Thank you for submitting your amendment requesting the following changes:

1) To make changes to the collection protocol: The ankle-foot orthotic will always be worn on the right leg. An ankle-foot orthotic acclimatization period will be added before the start of the data collection. During this period the participant will try each of the conditions until they say that they arecomfortable.

2) To modify the experimental conditions: Five experimental conditions will be collected: without AFO, with AFO (with no plantar flexion or restrictions), three experimental conditions with increasingplantar flexion angle up to a maximum of 50-degrees. During the three plantar flexion conditions, ankle dorsi flexion will be restricted to 10 degrees.

3) To add questionnaires related to the participant's perception of stability and effort.

4) To extend the collection period to 3 minutes of walking per condition, in which the participant will walk back-and-forth across the lab. Data will be collected for 10 strides. The participant will continue walking until the end of the three-minute period after which they will rate their perceived stability and tiredness. After each condition, there will be a five-minute break, during which the data will be checked, if needed AFO will be changed for the next condition, and the participant can answer the questionnaires for stability and effort.

5) To make a change to instrumentation to place an additional accelerometer sensor on the rightshank.

6) Letter of Information/Consent Form (v. 2019/03/27).

7) Questionnaires (v. 2019/03/27).

By this letter, you have ethics approval for these changes. Good luck with your

research.

Sincerely,

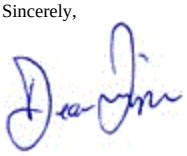

Dean Tripp, Ph. D. Chair
General Research Ethics Board

c.: Dr. Patrick Costigan, Supervisor

Appendix C

Efficiency and Stability Survey

Stability

Questionnaire was administered using a slider in Qualtrics, on a tablet

1. **Do you feel at risk of falling?**

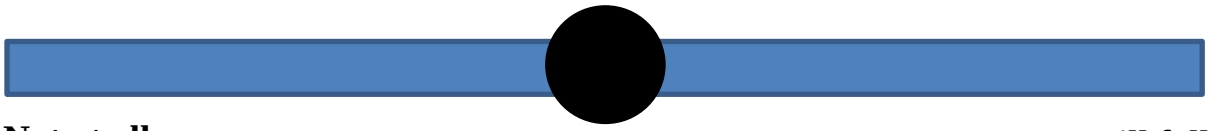

Not at all **Will fall**

2. **Are you worried about falling?**

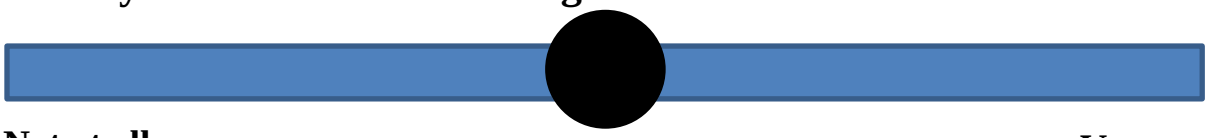

Not at all **Very worried**

3. **Compared to normal, how much more likely is it that you will fall?**

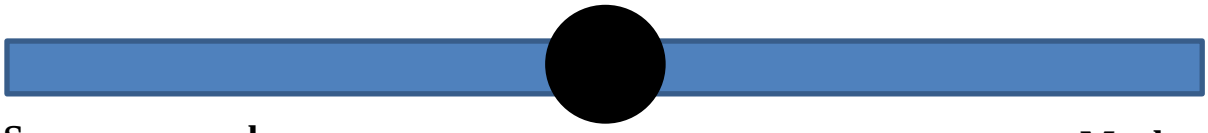

Same as normal **Much more likely**

Efficiency/Effort

Questionnaire was administered using a slider in Qualtrics, on a tablet

1. **How might you discribe your excersion (Borg)?**

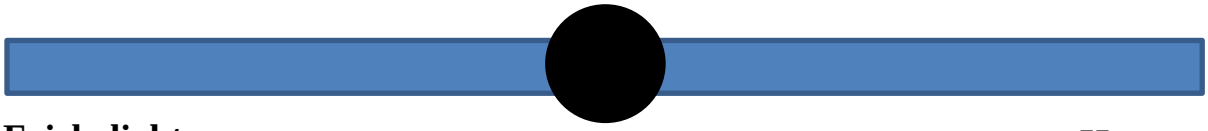

Fairly light (walking through grocery store)

Heavy (End of a sprint)

4. **Compared to normal, how tiring was this?**

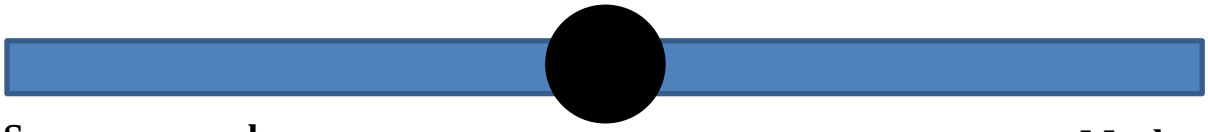

Same as normal

Much more tiring

Appendix D

Participant Information

Table D.1: Participant Information

Participant ID	Age	Sex	Limb Dominance	Height (cm)	Weight	Shoe size (M = Men's; W= Women's)	Notes
P1	25	M	R	178	82	10.5M	Right hip lower than left
P2	27	F	R	168	61	8W	Left ankle fracture at 14 years
P3	24	M	R	169	74	8M	concussion, dislocated finger, sprained ankle
P4	23	M	R	175	73	10.5M	mild left and right knee sprain (2yrs. And 4yrs ago)
P5	24	M	R	178	77	10M	left torn meniscus
P6	27	F	L	160	61	7W	spondylolisthesis L5 - Spinal fusion L4-S2, Left meniscus tear, concussions
P7	29	M	R	165	70	8.5M	Right ACL tear (2007), concussions
P8	28	M	R	170	68	8M	None
P9	23	M	R	178	75	10M	None
P10	22	F	R	160	42	7W	torn right ACL&MCL (2009), concussions, Achilles tendonitis (20014,2015)
P11	26	F	L	168	59	8W	ACL surgery (2015)
P12	24	M	R	181	79	10M	None
P13	23	F	R	163	64	8.5W	Right knee injury
P14	26	F	R	173	68	9.5W	None
P15	27	F	R	168	64	8W	Right hip lower than left

Appendix E

Static Ankle Angles (Participant X Condition)

Table E.1: Static Ankle Angles

Participant ID	Control	Zero AFO	Low Wedge	Medium Wedge	High Wedge
P1	100	95	100	105	118
P2	92	92	102	110	118
P3	95	95	103	110	118
P4	93	93	96	98	110
P5	95	93	112	104	118
P6	96	95	95	110	120
P7	95	95	100	105	118
P8	92	90	95	108	115
P9	105	95	105	113	118
P10	95	93	105	118	122
P11	90	92	98	102	113
P12	94	93	97	105	118
P13	95	95	101	105	118
P14	96	93	100	112	118
P15	95	92	96	105	115

Appendix F

Consent Form/Letter of Information

SCHOOL OF KINESIOLOGY AND HEALTH STUDIES (SKHS)

28 Division Street
Queen's University, Kingston, ON
K7L 3N6

Ethics Consent Form

Letter of Information

Investigating Efficiency and Stability of Gait using a Two Triaxial Accelerometer System

Dear Participant,

You are being invited to participate in a research study by Josh Davies (Graduate student, Queen's School of Kinesiology and Health Studies) and Dr. Patrick Costigan that examines how people move.

Your age, height and weight, level of physical activity, history of injury, and limb dominance will be recorded. During testing, a motion tracking system will track markers placed on your skin or over your clothing on your hips, knees, ankles, and feet as you walk across the lab. Two inertial measurement unit (IMU) sensors, one attatched to your low back and one attatched to a hat worn on your head will measure accelerations as you walk.

You will complete a total of 15 minutes of walking, ten trials in each of five experimental conditions: normal (no orthotic), normal (with orthotic set to zero gait deviations and restrictions), and three forced plantar flexion trials. The degree of plantar flexion will be manipulated using an ankle-foot orthotic on your right side. Before the start of data collection, you will be given the opportunity to try each one of the experimental conditions to ensure your comfort.

Risks of Participation
There is a minimal physical risk related to the forced change in your normal walking pattern. This alteration may increase the likelihood of falls. There are no direct benefits to you for taking part in this study.

Voluntary Participation and Withdrawal
Your participation in this study is completely voluntary and you can withdraw from the study at any time by informing the researcher during testing or by emailing the researcher at the email given below up to 3 months after data collection without penalty. If you withdraw, your data will be destroyed.

Confidentiality
All information obtained is strictly confidential and your identity will be protected as much as possible in all data analysis and publications. The data will be stored in an encrypted database that contains no identification information and retained indefinitely. Participant codes will be used to identify the data and no personal information will be stored in the database. Participant codes, names and contact information will be stored separately in a locked and secured location. We may ask permission to take photographs during testing to show the experimental set up. If you agree, images will be taken of your lower body. Should your face be photographed, it will be blurred in any presentation. You may refuse to be photographed and this will have no effect on your participation in the study.

The results from this research project may be used for publication. No identifiable personal information will be disseminated.

If at any time, you have questions or concerns related to your participation in this study, you can contact:

Josh Davies, Master's student, School of Kinesiology and Health Studies, Queen's University (613) 533-6000 ext.: 79019
Patrick Costigan, Ph.D. Associate Professor, School of Kinesiology and Health Studies, Queen's University (613) 533-6000 ext.: 79037

If you have any concerns related to ethics at any time, please contact the General Research Ethics Board (GREB) at 1-844-535-2988 (Toll free in North America) or at chair.GREB@queensu.ca.

Ethics Consent: Participant's Copy

Investigating Efficiency and Stability of Gait using a Two Triaxial Accelerometer System

This page is for the researchers to verify that you are willing to participate in the above study. By signing this page, you are declaring the following:

- You were given a verbal presentation about the above-mentioned research study
- You were given a copy of the Information and Ethics Consent Letter to read and keep
- You realize you can withdraw at any time without penalty or coercion
- You can contact any of people in this letter if you have questions, concerns or complaints
- You realize that your data will be kept confidential.
- You do not wave your legal rights nor release the investigator(s) and sponsors from their legal and professional responsibilities.

(Please sign and keep this page for your own records)

_____ _____

Print your Name Date

_____

Signature of Participant

_____ _____

Principal Investigator Date

Please initial here if you are willing to permit photos to be taken _____.

Witness Initials: _____

Thank you.

Josh Davies, School of Kinesiology and Health Studies, Queen's University

Ethics Consent: Researcher's Copy

Investigating Efficiency and Stability of Gait using a Two Triaxial Accelerometer System

This page is for the researchers to verify that you are willing to participate in the above study.

By signing this page, you are declaring the following:

- You were given a verbal presentation about the above-mentioned research study
- You were given a copy of the Information and Ethics Consent Letter to read and keep
- You realize you can withdraw at any time without penalty or coercion
- You can contact any of people in this letter if you have questions, concerns or complaints
- You realize that your data will be kept confidential.
- You do not wave your legal rights nor release the investigator(s) and sponsors from their legal and professional responsibilities.

(Please sign and return this page ONLY to the researchers)

_____ _____
Print your Name Date

_____
Signature of Participant

_____ _____
Principal Investigator Date

Please initial here if you are willing to permit photos to be taken _____.

Witness Initials: _____

Thank you.

Josh Davies, School of Kinesiology and Health Studies, Queen's University

Appendix G

Data Collection Sheet

Participant ID: _____ Date and time:

_____

- ☐ Consent Form/Letter of Information

Demographics	
Age: _____	Height (cm): _____
Gender: _____	Weight (kg): _____
Dominant limb: _____	Shoe size : _____ M/F

Injury History:

Sensor Placement/Settings:	
☐ Head ☐ CoM	☐ Logging ☐ Acceleration ☐ Gravity

Marker Placement:	
☐ Left foot (two markers) ☐ Left shank (two markers) ☐ Right foot (two markers ☐ Right shank (two markers) Total markers: 13	☐ Thigh (greater trochanters, lateral femoral condyle) ☐ Marker on each sensor ☐ Heel markers

Collection:
☐ Set path ☐ Static for each trial ☐ Initial AFO acclimatization (before each trial) ☐ Random condition order: _____ ☐ 3-minute timer from start of collection ☐ "Pause, go, pause, turn, pause, go…'

Condition info:	
☐ Normal ☐ Zero AFO	☐ Condition 1 ☐ Condition 2 ☐ Condition 3

Measured ankle angle:

Condition	*Angle*
1	
2	
3	
4	
5	

Condition 1:

Time:

Trial	*Notes*
1	
2	
3	
4	

5	
6	
7	
8	
9	
10	

Condition 2:

Time:

Trial	*Notes:*
1	
2	
3	
4	
5	
6	
7	
8	

9	
10	

Condition 3:

Time:

Trial	*Notes*
1	
2	
3	
4	
5	
6	
7	
8	
9	
10	

Condition 4:

Time:

Trial	*Notes*
1	
2	
3	
4	
5	
6	
7	
8	
9	
10	

Condition 5:

Time:

Trial	*Notes*
1	
2	
3	
4	
5	
6	
7	
8	
9	
10	

Appendix H

Post-Hoc Power Analyses (G-Power)

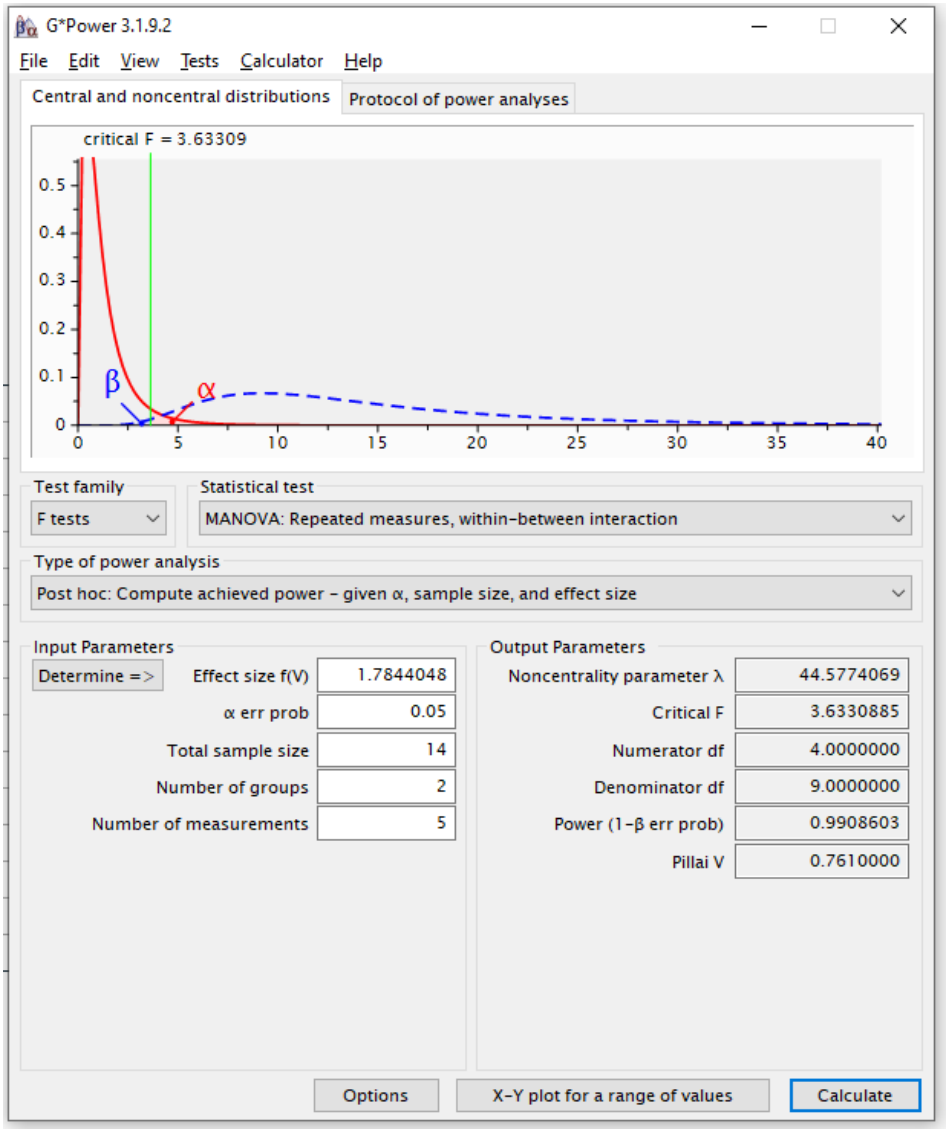

Figure H.1: Screen-capture of G*power, power analysis for the repeated measures MANOVA effect of condition on efficiency measures.

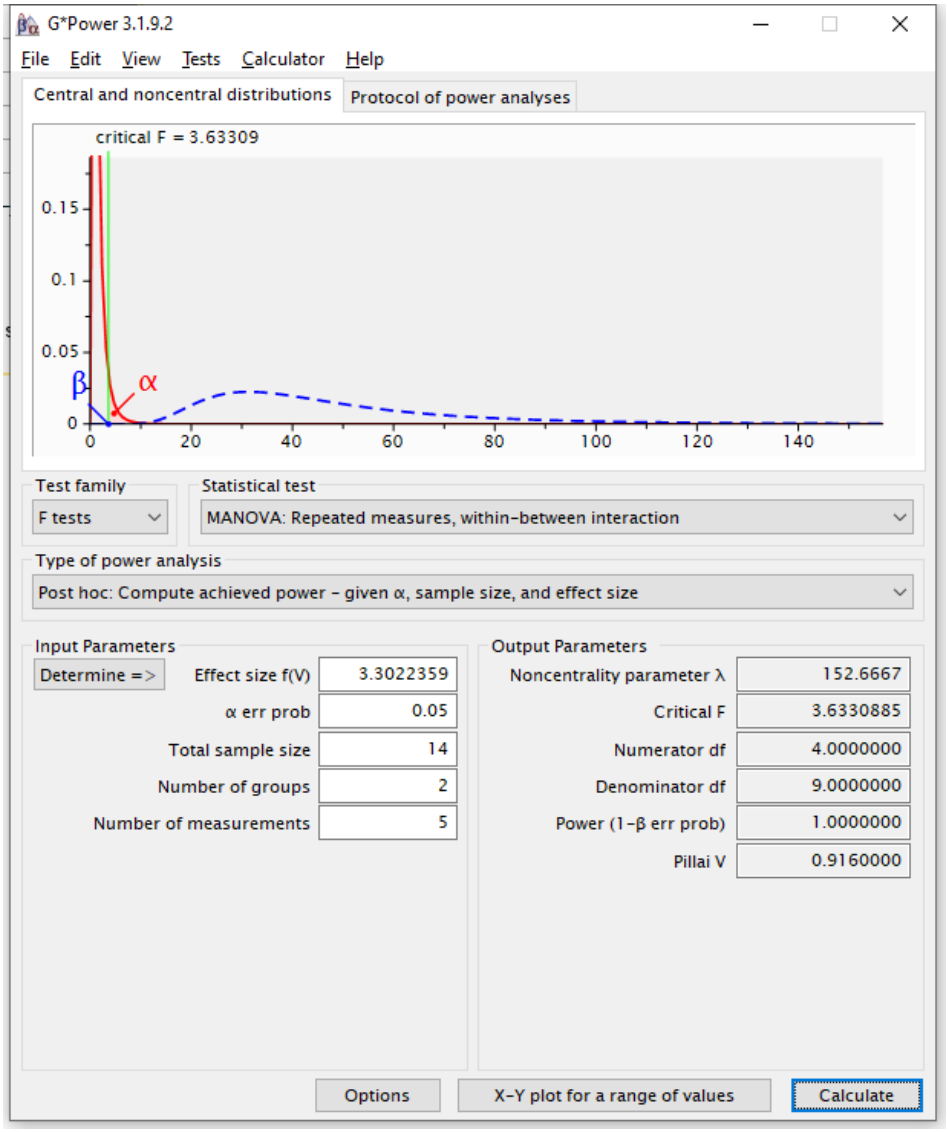

Figure H.2: Screen-capture of G*power, power analysis for the repeated measures MANOVA effect of condition on the harmonic ratios of the low back.

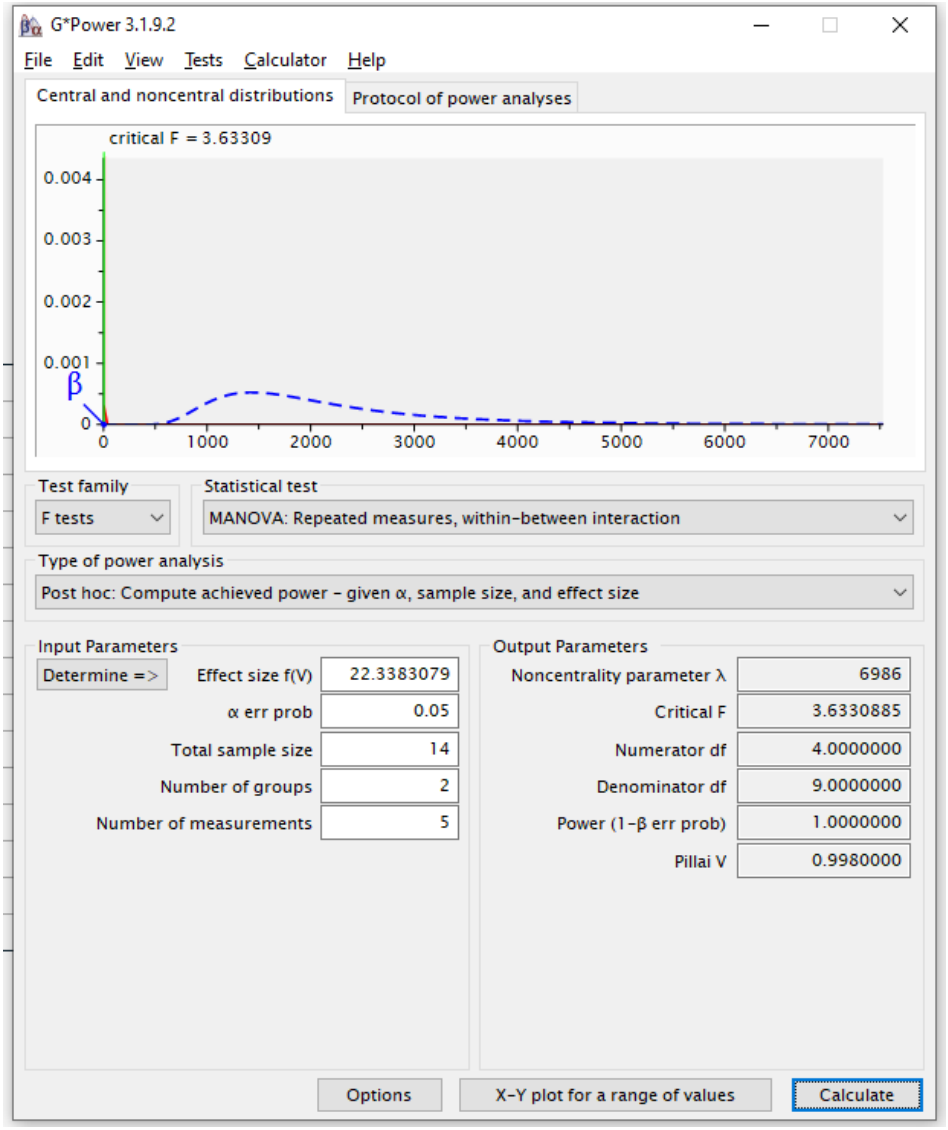

Figure H.3: Screen-capture of G*power, power analysis for the repeated measures MANOVA effect of condition on the harmonic ratios of the head.

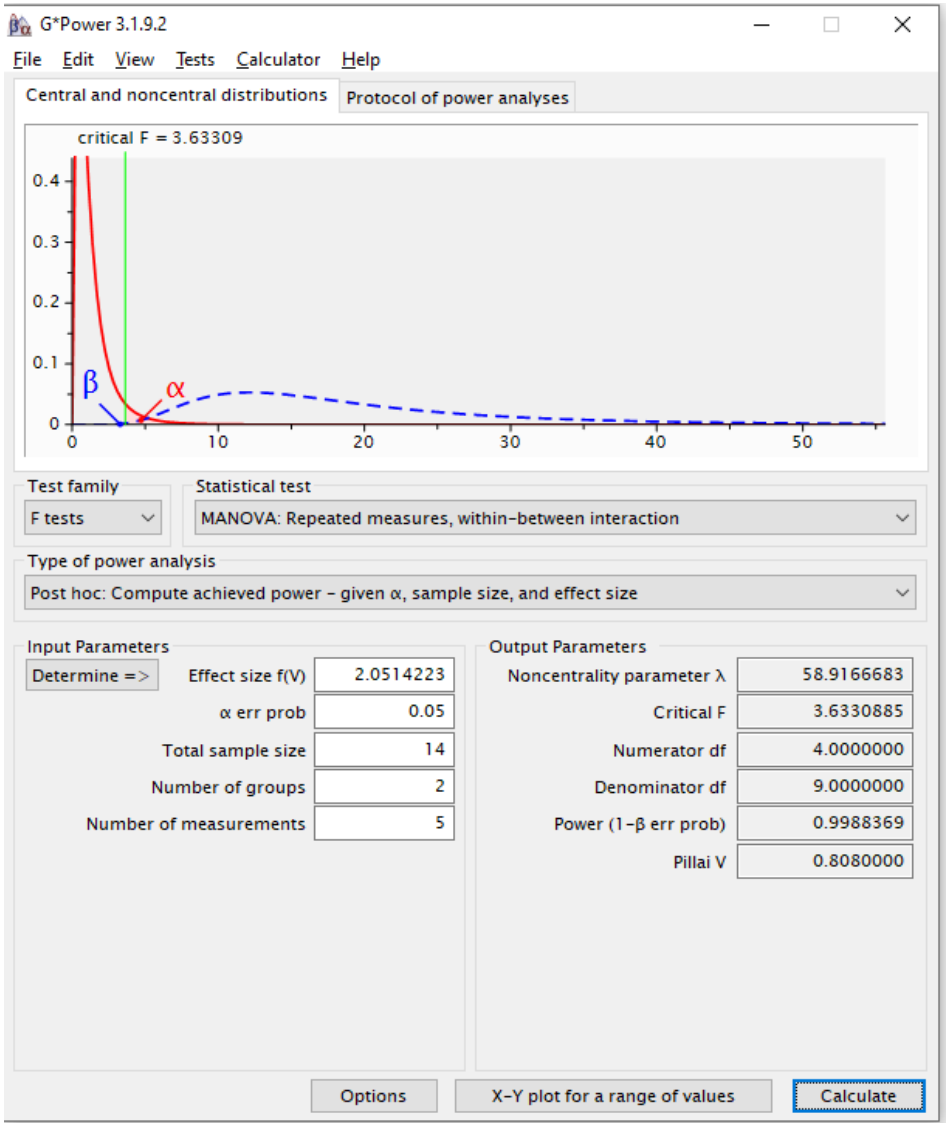

Figure H.4: Screen-capture of G*power, power analysis for the repeated measures MANOVA effect of condition on the percent attenuation values.